PLOS GENETICS

RESEARCH ARTICLE

Integration of cooperative and opposing molecular programs drives learning-associated behavioral plasticity

Jessica C. Nelson[1,2]*, **Hannah Shoenhard**[1], **Michael Granato**[1]*

1 Department of Cell and Developmental Biology; University of Pennsylvania, Perelman School of Medicine; Philadelphia, Pennsylvania, United States of America, **2** Department of Cell and Developmental Biology; University of Colorado Anschutz Medical Campus, Aurora, Colorado, United States of America

* jessica.c.nelson@cuanschutz.edu (JCN); granatom@pennmedicine.upenn.edu (MG)

Citation: Nelson JC, Shoenhard H, Granato M (2023) Integration of cooperative and opposing molecular programs drives learning-associated behavioral plasticity. PLoS Genet 19(3): e1010650. https://doi.org/10.1371/journal.pgen.1010650

Editor: Cecilia Moens, Fred Hutchinson Cancer Research Center, UNITED STATES

Received: May 31, 2022

Accepted: February 2, 2023

Published: March 27, 2023

Data Availability Statement: All original code is available in S1 Code. All relevant data are within the manuscript and its Supporting information files (S1 Data).

Funding: This work was supported by grants to M. G.: NIH National Institute of Neurological Disorders and Stroke, R01NS118921 and J.N.: NIH National Institute of Neurological Disorders and Stroke, K99NS111736 and R00NS111736. The funders had no role in study design, data collection and analysis, decision to publish, or preparation of the manuscript.

Abstract

Habituation is a foundational learning process critical for animals to adapt their behavior to changes in their sensory environment. Although habituation is considered a simple form of learning, the identification of a multitude of molecular pathways including several neurotransmitter systems that regulate this process suggests an unexpected level of complexity. How the vertebrate brain integrates these various pathways to accomplish habituation learning, whether they act independently or intersect with one another, and whether they act via divergent or overlapping neural circuits has remained unclear. To address these questions, we combined pharmacogenetic pathway analysis with unbiased whole-brain activity mapping using the larval zebrafish. Based on our findings, we propose five distinct molecular modules for the regulation of habituation learning and identify a set of molecularly defined brain regions associated with four of the five modules. Moreover, we find that in module 1 the palmitoyltransferase Hip14 cooperates with dopamine and NMDA signaling to drive habituation, while in module 3 the adaptor protein complex subunit Ap2s1 drives habituation by antagonizing dopamine signaling, revealing two distinct and opposing roles for dopaminergic neuromodulation in the regulation of behavioral plasticity. Combined, our results define a core set of distinct modules that we propose act in concert to regulate habituation-associated plasticity, and provide compelling evidence that even seemingly simple learning behaviors in a compact vertebrate brain are regulated by a complex and overlapping set of molecular mechanisms.

Author summary

Habituation is an evolutionarily ancient form of learning in which responses to repeated stimuli decline over time. While seemingly simple, habituation is nevertheless regulated by multiple molecular mechanisms. This surprising complexity led us to ask: do these diverse mechanisms act independently of one another or do they work in the same pathways to drive habituation? To answer this question, we mapped how individual regulators of habituation alter activity throughout the brain and perturbed habituation-regulating

Competing interests: The authors have declared that no competing interests exist.

molecular mechanisms in combination to see if they act in the same or different pathways. Our experiments grouped eight molecular regulators of habituation into five different pathways with their own brain activity signatures, indicating that multiple independent pathways regulate even simple learning mechanisms.

Introduction

Learning enables animals to modify their responses to stimuli based on prior experience. One of the simplest forms of learning is a non-associative plasticity mechanism termed habituation, which is defined by a gradual decrease in responding to repeated stimuli [1–3]. Habituation represents a foundation for more complex forms of behavioral plasticity and is observed in all animals. Habituation learning is also a pervasive feature of the nervous system, regulating response rates to stimuli spanning sensory modalities and including complex responses such as fear responses and feeding [4–6]. We previously established larval zebrafish as a model to study short term habituation learning [7]. In response to a sudden acoustic stimulus zebrafish perform a stereotyped acoustic startle response (ASR), comprised of a short-latency C-bend (SLC) escape response regulated by well-described hindbrain circuitry [8–10]. Repeated acoustic stimuli modulate sensory thresholds and result in habituation learning characterized by a gradual decline in response frequency [7,11–14]. Although this process appears simple at first glance, previous work revealed that at least long-term habituation learning is regulated by multiple mechanisms that operate on distinct time scales [2,15]. Similarly, numerous molecular-genetic mechanisms also regulate short-term habituation learning [16–25]. Moreover, pharmacological screens have identified multiple neurotransmitter and neuromodulatory systems contributing to habituation [7]. Despite their known relevance for learning, how individual habituation-regulatory pathways relate to one another, whether they act sequentially or regulate habituation learning in parallel, and whether they are distributed over multiple brain areas or function within a common circuit is unclear.

Here, we utilize at set of well-defined habituation mutants in conjunction with pharmacological agents to determine whether individual molecular regulators of habituation function together with or in parallel to habituation-relevant neurotransmitter systems. To complement this pharmacogenetic approach, we then performed unbiased whole-brain imaging to define activity signatures for each independent pharmacological or genetic manipulation, in order to identify candidate brain regions in which habituation-regulatory modules exert their function. We propose five distinct molecular-circuit modules that regulate habituation. Module 1 consists of the palmitoyltransferase Hip14, as well as NMDA and dopamine signaling, while module 2 consists of Hip14 and one of its identified substrates, the voltage-gated Potassium channel subunit Kv1.1. Module 3 consists of the *pregnancy-associated plasma protein A* (PAPP-AA) and the AP2 adaptor complex subunit AP2S1, which both act to oppose dopamine signaling. Glycine signaling constitutes module 4, and the *voltage dependent calcium channel alpha2/delta subunit 3* gene (*cacna2d3*) defines module 5. Two of these modules reveal a critical role for dopamine signaling in the bi-directional modulation of habituation learning. Specifically, while the palmitoyltransferase Hip14 cooperates with neurotransmitter signaling through NMDA and dopamine receptors to drive habituation (module 1), the AP2 adaptor complex subunit AP2S1 promotes behavioral plasticity by opposing dopamine signaling (module 3). Moreover, we find that three of the proposed habituation-regulatory modules intersect functionally (modules 1, 2 and 3), while modules 4 and 5 appear functionally independent

from each other and from the other three interconnected modules, suggesting multiple habituation-regulatory mechanisms that act in parallel.

Importantly, habituation learning and baseline behavioral response thresholding are tightly linked. Human disorders that impact habituation learning often co-influence baseline sensitivity to stimuli [26]. Although our screens for pharmacological and genetic regulators of habituation learning additionally identified regulators that impact solely habituation or solely hypersensitivity, all of the mutants that we examine here impact both processes. Whether these processes are interdependent or regulated in parallel is difficult to disentangle. Therefore, although we refer to these genes as regulators of habituation learning, our findings may additionally be relevant for understanding how animals establish response thresholds *in vivo*.

Taken together, our findings highlight the strength of an integrative approach combining genetic and pharmacological manipulation of habituation learning with unbiased whole-brain activity mapping and reveal a more complete picture of the molecular and circuit mechanisms that drive vertebrate habituation learning.

Results

A reduced-intensity habituation assay to uncover pharmacogenetic interactions

From an unbiased genetic screen we previously identified a set of five genes required for habituation learning [25,27–29]. To determine whether the identified molecular and circuit mechanisms regulate habituation learning independently of each other, or whether these genetic mechanisms converge at a common bottleneck, we set out to perform pathway analysis by exposing habituation mutants to pharmacological inhibitors of habituation-regulatory neurotransmitter signaling pathways. We reasoned that genetic and pharmacological manipulations that impinge upon components of independent or parallel pathways would enhance habituation deficits while multiple insults to components of a common pathway would fail to produce additive deficits. However, impeding our ability to perform such analyses, we observed that genetic mutations that affect habituation learning, such as presumptive null mutations in the *zinc finger DHHC-type palmitoyltransferase gene zdhhc17*, encoding the palmitoyltransferase Hip14, result in a near complete loss of habituation at our standard stimulus intensities of 35.1dB (Fig 1A and 1B) [28]. This ceiling effect interferes with the ability to detect additive habituation learning deficits, preventing us from detecting a further reduction in habituation and thus preventing us from interpreting the results of the proposed pharmacogenetic pathway analysis. We therefore wondered whether reducing stimulus intensity might provide a more sensitive assay in which mutant animals retain some capacity for habituation, and application of a pharmacological inhibitor of habituation learning might reveal more severe deficits. Consistent with previous findings that habituation learning is modulated by stimulus intensity [2], we find that although still impaired relative to their siblings, *hip14* mutant animals are capable of habituation learning under conditions of reduced stimulus intensity (i.e. 0.4dB-25.6dB, Fig 1C–1G). Moreover, these data reveal that presumptive null mutations in *hip14* fail to fully abolish habituation, and that when presented with lower intensity stimuli *hip14* mutant animals are capable of habituation learning, albeit at a reduced level relative to their siblings. We conclude that at lower intensity, further habituation impairments in *hip14* mutants induced by pharmacological inhibitors of learning might be readily detectable. We therefore selected 19.8dB for our reduced-intensity habituation assay and utilized this stimulus intensity to test five genetic mutants in combination with individual inhibitors of three neurotransmitter systems.

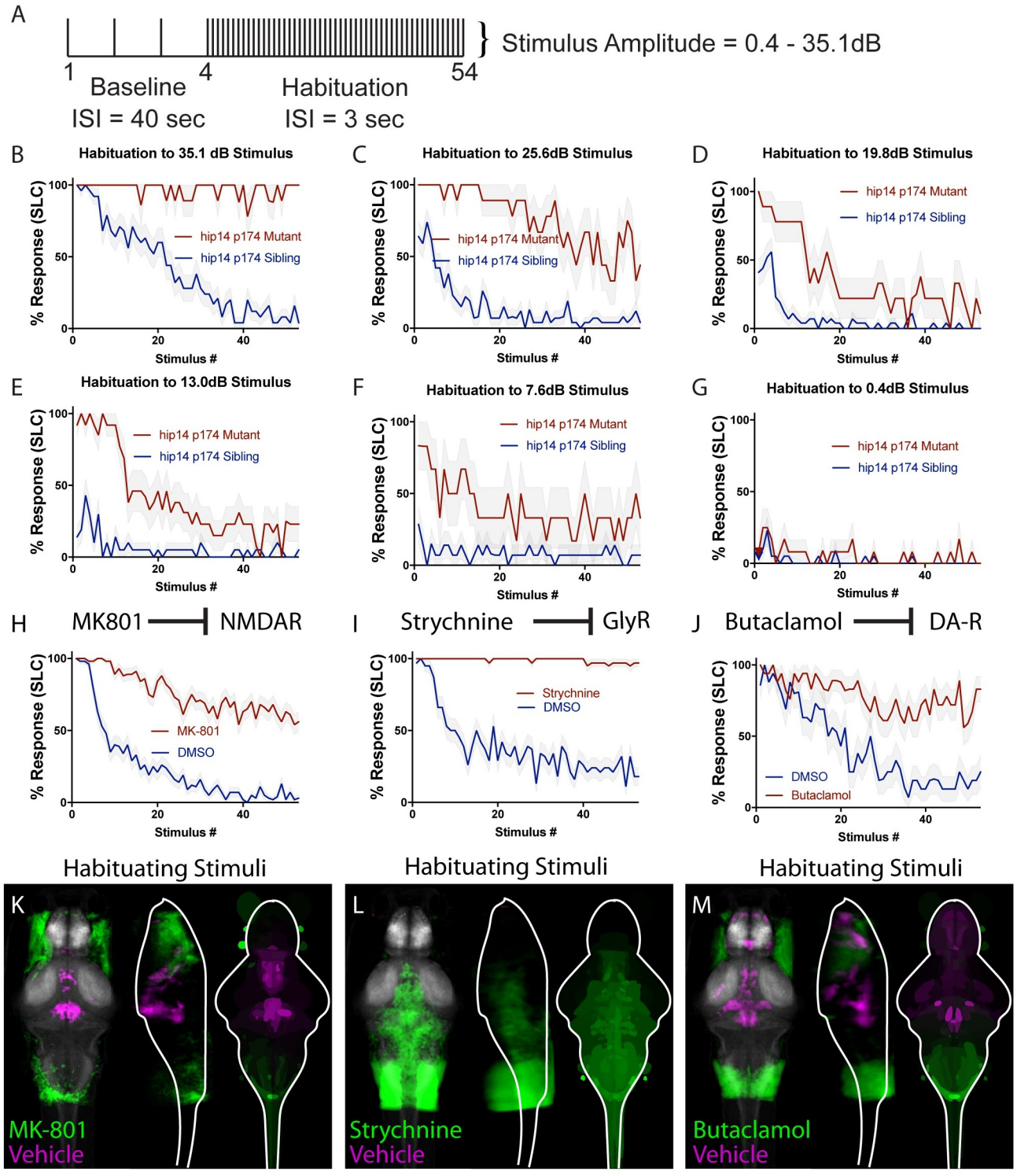

Fig 1. Reduced-intensity habituation assay and unbiased whole-brain imaging to examine impact of pharmacological inhibitors of habituation learning. **(A)** Stimulus paradigm used. ISI for baseline phase is 40 seconds, ISI for habituation phase is 3 seconds. **(B)** *hip14* mutants exhibit a complete failure to habituate to 35.1 dB acoustic stimuli. **(C-G)** Reduction in stimulus intensity as indicated results in a gradual increase in the ability of *hip14* mutants to habituate. **(H)** MK-801 is an NMDA inhibitor that strongly reduces habituation learning in 5-day old zebrafish larvae (n = 58 DMSO-treated, n = 57 MK-801-treated, stimulus intensity = 35.1dB). **(I)** Strychnine is a glycine receptor antagonist that strongly reduces habituation learning in 5-day old zebrafish larvae (n = 38 DMSO-treated, n = 38 Strychnine-treated, stimulus intensity = 35.1dB). **(J)** Butaclamol is a dopamine inhibitor that strongly reduces habituation learning in 5-day old zebrafish larvae (n = 16 DMSO-treated, n = 18 Butaclamol-treated, stimulus intensity = 35.1 dB). **(K-M)**

Regions upregulated by the specified drug treatment under "Habituating Stimuli" conditions are indicated in green; regions upregulated in the vehicle (can also be interpreted as downregulated in drug-treated) are indicated in magenta. In all images, the left panel is a summed z-projection of the whole-brain activity changes. The middle panel is a summed x-projection of the whole brain activity changes. The right panel is a z-projection of the analyzed MAP-map. Molecular targets of pharmacological agents are indicated with diagrams above each column. See S1 Fig for brain activity maps under "No Stimulus" condition and "Non-Habituating Stimuli" condition. Also see S1–S3 Tables for ROIs identified in the experiments presented as well as in an independent replicate of each drug condition.

https://doi.org/10.1371/journal.pgen.1010650.g001

Pharmacological inhibitors of habituation learning produce distinct patterns of neuronal activity

For the pharmacogenetic pathway analysis we selected the NMDA receptor inhibitor MK-801, the glycine receptor inhibitor Strychnine, and the dopamine receptor inhibitor Butaclamol. As previously reported, in 5-day old larval zebrafish, application of MK-801 results in significant impairments in habituation learning (Fig 1H) [7,30]. Whereas vehicle-exposed animals rapidly learn to ignore repeated acoustic stimuli, i.e. habituate, animals exposed acutely to the NMDA inhibitor continue to respond at a high rate (they fail to habituate). Similar effects are observed when animals are exposed to Strychnine (Fig 1I) or Butaclamol (Fig 1J) [7]. Despite their similar effects on habituation learning, we hypothesized that given their regulation of different neurotransmitter systems, these pharmacological agents might regulate habituation through distinct effects on neuronal activity. In order to broadly assess brain activity signatures associated with each pharmacological treatment, we performed unbiased whole-brain activity mapping using the MAP-mapping technique [31]. This approach uses immunohistochemistry to measure ratios between phosphorylated ERK (extracellular signal-regulated kinase) and total ERK as a readout for neural activity in the minutes preceding fixation. We performed this assay for each of the three pharmacological inhibitors under three different acoustic stimulation conditions: "No Stimuli," "Non-Habituating Stimuli," and "Habituating Stimuli." The resulting activity maps highlight brain areas whose activity is greater in drug-treated relative to vehicle-exposed animals (green = up-regulated in drug-treated) and brain areas whose activity is greater in vehicle-exposed relative to drug-treated animals (magenta = down-regulated in drug-treated). We find that each pharmacological agent produces a distinct activity pattern (Fig 1K–1M and S1A–S1F Fig). Furthermore we find that the distinct patterns of activity induced by each inhibitor of habituation learning are largely maintained across stimulation conditions (Fig 1K–1M and S1A–S1F Fig, S1 Table). In particular, MK-801 suppresses activity within the subpallium, habenula, and hypothalamus (activity maps indicate increased activity in vehicle-treated relative to MK-801-treated: Fig 1K, S1A and S1D Fig), Strychnine produces widespread hyperactivation (Fig 1L, S1B and S1E Fig), and Butaclamol treatment results in hindbrain hyperactivation and forebrain and diencephalic suppression relative to vehicle controls (Fig 1M, S1C and S1F Fig). Our results that differences between inhibitor conditions, but not stimulation conditions were readily detected reflects the design of our experiments, which were optimized to detect differences between drug conditions at the expense of sensitivity to differences in stimulation conditions. Together, these data are consistent two scenarios: (1) that the neurotransmitter systems that regulate habituation impinge upon different sets of circuit loci, which separately regulate learning, and/or (2) that their effects on habituation are mediated through the limited regions that show overlapping activity changes.

Hip14 acts through NMDA and dopamine signaling and mutants show broad hyperactivity of neuronal circuits

Having developed a more sensitive habituation assay, and having established that pharmacological inhibitors of habituation impinge upon activity within distinct brain regions, we set out

to perform our pharmacogenetic analysis to examine all possible interactions between three neurotransmitter signaling inhibitors and five habituation mutants. We first tested whether Hip14 and NMDA receptors act together to regulate habituation learning by exposing mutant and sibling animals to either vehicle (DMSO) or the NMDA inhibitor MK-801 and then performing the reduced-intensity habituation assay (Fig 1A and 1D). We found that while MK-801 severely reduced habituation in sibling animals, the same pharmacological manipulation in *hip14* mutant animals did not further reduce habituation learning (Fig 2A). This is consistent with a model in which Hip14 and NMDA act in a common pathway to drive habituation learning. When we plotted response frequency versus stimulus number in order to analyze the kinetics of habituation learning (learning curves), we found that compared to MK-801-treated mutants, sibling animals treated with MK-801 exhibited more severe habituation deficits (Fig 2B). This raises the possibility that compensatory, NMDA-independent plasticity mechanisms are upregulated in *hip14* mutant animals. When we performed the same protocol in the presence of the glycine-receptor inhibitor Strychnine, we observed further reductions in habituation in both siblings and *hip14* mutants, consistent with the idea that the regulation of habituation learning involves independent roles for glycine and Hip14 (Fig 2C and 2D). Finally, we performed our reduced-intensity habituation assay in the context of the dopamine receptor inhibitor Butaclamol. Here we found that in sibling animals dopamine receptor inhibition significantly impaired habituation. In contrast, in *hip14* mutant animals the same manipulation did not reduce habituation learning (Fig 2E and 2F). Taken together, our data provide strong evidence that Hip14 acts in a common pathway with dopamine and NMDA receptor signaling yet independently of glycine receptor signaling to drive habituation learning.

In light of the finding that Hip14, dopamine, and NMDA signaling act in a common pathway to regulate habituation, we wondered whether *hip14* mutant animals might display similar activity signatures to those obtained from larvae treated with NMDA or dopamine inhibitors. To address this question, we performed whole-brain activity mapping in animals lacking *hip14*, analyzed the resultant MAP-maps, and compared them with those obtained from NMDA and dopamine inhibitor treated animals. In *hip14* mutant brains we observed broad hyperexcitability across the forebrain and hindbrain (Fig 2G–2I). Despite this being a distinct pattern from that observed in NMDA- and dopamine-inhibited animals, we observed commonalities in the activity signatures. In particular, activity in the diencephalon was reduced, and a handful of rhombencephalic areas were upregulated by all three manipulations (Fig 2G–2I, S1 Table). These overlapping activity changes, observed across multiple treatments, represent potential habituation-regulating loci through which these putative regulatory modules may exert their function.

Kv1.1 mutants exhibit a unique activity signature and Kv1.1 acts independently of NMDA, glycine, and dopamine signaling

We have previously shown that Hip14 acts in part through the voltage-gated Potassium channel subunit Kv1.1, which is encoded by the *potassium voltage-gated channel*, *shaker-related subfamily member 1a gene*, *kcna1a* [28]. We performed pharmacogenetic pathway analysis in *kcna1a* mutants and found that in contrast to *hip14* mutants, *kcna1a* mutants did not show significant habituation deficits in our modified habituation assay. Nonetheless, we hypothesized that if a given neurotransmitter pathway was disrupted in these mutants, it would still likely show an interaction in our assay.

However, we found no evidence that Kv1.1 functions in a pathway with NMDA receptor signaling. Rather, the NMDA receptor inhibitor MK-801 induced significant habituation

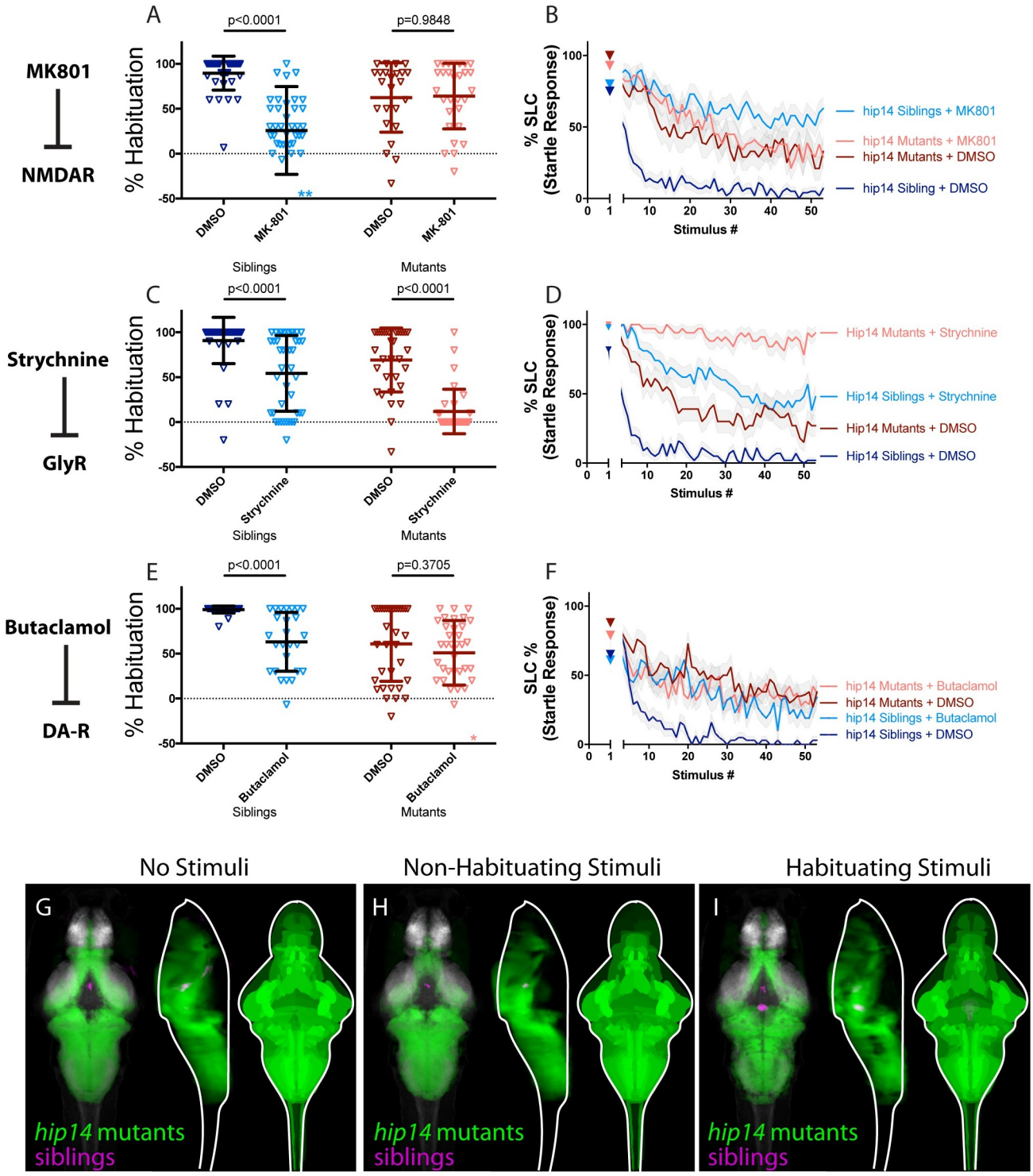

Fig 2. Hip14 acts through NMDA and dopamine signaling and produces broad hyperactivity of neuronal circuits. (A-B) MK-801 impairs habituation learning in siblings, ($p<0.0001$ Sidak's test for multiple comparisons, n = 38 DMSO, n = 38 MK-801), but does not enhance habituation learning deficits observed in *hip14* mutant larvae ($p = 0.9848$, n = 24 DMSO, n = 29 MK-801, $p<0.0001$ indicates significant interaction between drug treatment and genotype; these and all subsequent statistical analyses use Two-way ANOVA with Sidak's multiple comparisons test unless otherwise indicated). **indicate sibling+MK801 individuals with % hab values below y-axis limit at -100% and -180%. **(C-D)** Strychnine significantly enhances habituation learning deficits observed in *hip14* mutant larvae, indicating that glycine signaling and *hip14* may act within parallel molecular or circuit pathways to regulate habituation learning ($p<0.0001$, n = 40 DMSO-siblings, n = 42 Strychnine-siblings, n = 32 DMSO-mutants, n = 32 Strychnine-mutants, $p = 0.0639$

indicates non-significant interaction between drug treatment and genotype). **(E-F)** Butaclamol impairs habituation learning in siblings ($p<0.0001$, n = 33 DMSO, n = 26 Butaclamol), but does not enhance habituation learning deficits observed in *hip14* mutant larvae ($p = 0.3705$, n = 34 DMSO, n = 35 Butaclamol, $p = 0.0239$ indicates significant interaction between drug treatment and genotype), indicating that dopamine receptor signaling and *hip14* may act within the same molecular or circuit pathway to regulate habituation. *indicates a mutant+butaclamol individual with % hab value below y-axis limit at -60%. **(G-I)** Regions upregulated in *hip14* mutants are indicated in green; regions upregulated in siblings (can also be interpreted as downregulated in *hip14* mutants) are indicated in magenta. In all images, the left panel is a summed z-projection of the whole-brain activity changes. The middle panel is a summed x-projection of the whole brain activity changes. The right panel is a z-projection of the analyzed MAP-map. Patterns of neuronal activity are similar between "No Stimuli" vs "Non-Habituating Stimuli" vs. "Habituating Stimuli" (restricted diencephalic downregulation of activity; nearly global upregulation of activity across the telencephalon, diencephalon, and rhombencephalon). See also S1–S3 Tables for ROIs up- and down-regulated in each condition, as well as in independent replicates.

https://doi.org/10.1371/journal.pgen.1010650.g002

deficits in both *kcna1a* siblings and mutants (Fig 3A and 3B). Similarly, glycine receptor inhibition induced significant habituation learning deficits in both *kcna1a* mutants and siblings (Fig 3C and 3D). Finally, we observed significant enhancement of habituation learning deficits through inhibition of dopamine signaling in both *kcna1a* siblings and mutants (Fig 3E and 3F). Taken together, these data are consistent with a model in which *kcna1a* acts independently of NMDA, dopamine, and glycine receptor signaling to regulate habituation learning.

Next, we performed whole-brain activity mapping to identify where *kcna1a* might exert its function, and to assess whether its activity signature might overlap with that of other regulators of habituation. We found a remarkably specific and unique pattern of activity induced by the loss of *kcna1a*. In particular, two populations known to express Kv1.1 [28,32] and involved in the execution of the escape response were found to be hyperactive: spiral fiber neurons and RoM3 excitatory reticulospinal (V2a) neurons (Fig 3G–3I). We previously showed that Kv1.1 requires Hip14 for proper synaptic localization and hence likely acts downstream of Hip14 to regulate habituation learning. Consistent with these findings, we now find that the same populations that are hyperactive in *kcna1a* mutants are also hyperactive in *hip14* mutants in all conditions except for one (Non-Habituating Stimuli Replicate 2 of 3). Moreover, the observation that activity changes are more restricted in *kcna1a* mutant brains compared to those observed in *hip14* mutant brains is consistent with our prior observation of more severe habituation learning deficits in *hip14* mutants as compared to *kcna1a* [28]. These data lend further support to our hypothesis that Hip14 acts through other substrates besides Kv1.1 to regulate habituation. Combining these results with the findings of our pharmacogenetic analysis, we conclude that Kv1.1 may function in a restricted set of hindbrain neurons to carry out NMDA- and dopamine-independent functions downstream from Hip14.

PAPP-AA promotes habituation by limiting endogenous dopamine signaling

The previous genetic screen additionally identified the *pregnancy-associated plasma protein A* (*pappaa*) gene as a critical regulator of habituation learning. PAPP-AA has been shown to act through regulation of Insulin Growth Factor Receptor (IGFR) signaling to regulate habituation, yet it is unknown whether PAPP-AA interacts with any of the other identified habituation regulatory pathways. In order to investigate this question, we also performed pharmacogenetic pathway analysis in *pappaa* mutants. Compared to DMSO-treated *pappaa* mutants, application of MK-801 or Strychnine to mutant animals resulted in further reduction of habituation learning, providing compelling evidence that PAPP-AA promotes habituation learning independent of NMDA (Fig 4A and 4B), and glycine receptor signaling (Fig 4C and 4D). In contrast, treatment of *pappaa* mutants with the dopamine receptor antagonist Butaclamol failed to enhance habituation deficits in *pappaa* mutants when compared to DMSO treated mutants, and in fact trended toward ameliorating habituation deficits in *pappaa*

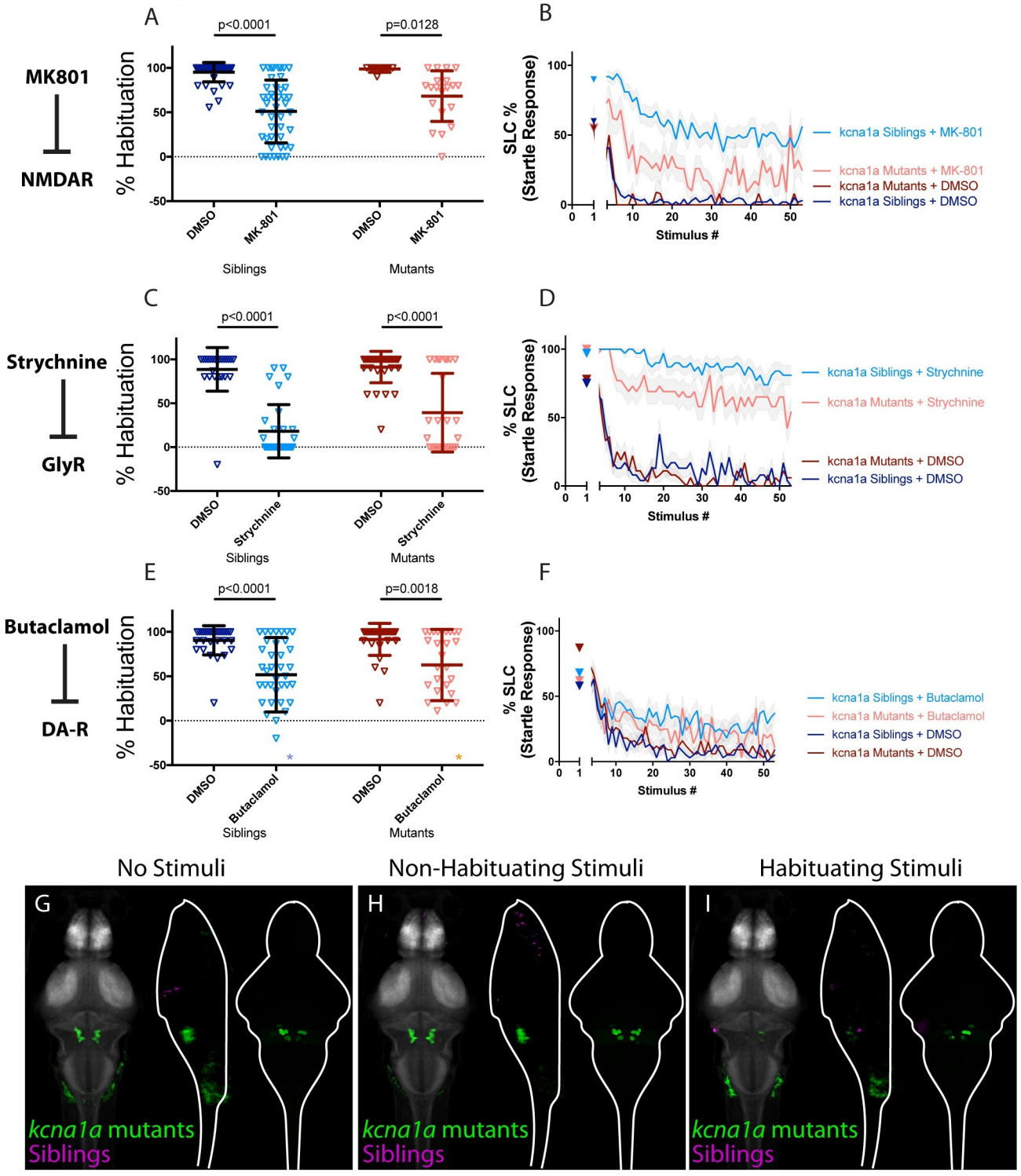

Fig 3. Kv1.1 exhibits a unique activity signature and acts independently of NMDA, glycine, and dopamine signaling. (A-B) MK-801 significantly enhances habituation learning deficits in *kcna1a* mutants and siblings ($p<0.0001$, n = 42 DMSO-siblings, n = 46 MK-801-siblings, $p = 0.0128$, n = 8 DMSO-mutants, n = 20 MK-801 mutants, $p = 0.2628$ indicates non-significant interaction between drug treatment and genotype). **(C-D)** Strychnine significantly enhances habituation learning deficits in *kcna1a* mutants and siblings ($p<0.0001$, n = 24 DMSO-siblings, n = 31 Strychnine-siblings, $p<0.0001$, n = 35 DMSO-mutants, n = 26 Strychnine-mutants, $p = 0.1063$ indicates non-significant interaction between drug treatment and genotype). **(E-F)** Butaclamol significantly enhances habituation learning deficits in *kcna1a* mutants and siblings ($p<0.0001$, n = 30 DMSO-siblings, n = 37 Butaclamol-siblings, $p = 0.0018$, n = 30 DMSO-mutants, n = 27 Butaclamol-mutants, $p = 0.3942$ indicates non-significant interaction between drug

treatment and genotype). *indicate a sibling+butaclamol and a mutant+butaclamol individual with % hab values below y-axis limit at -100% and -60% respectively. **(G-I)** Regions upregulated in *kcna1a* mutants are indicated in green; regions downregulated in *kcna1a* mutants are indicated in magenta. In all images, the left panel is a summed z-projection of the whole-brain activity changes. The middle panel is a summed x-projection of the whole brain activity changes. The right panel is a z-projection of the analyzed MAP-map. We observed similar patterns of neuronal activity induced by "no stimuli" vs "non-habituating stimuli" vs. "habituating stimuli": highly restricted upregulation of activity in the spiral fiber neuron clusters as well as in V2A (including Rom3) neurons. See also S1–S3 Tables for ROIs up- and down-regulated in each condition, as well as in independent replicates.

https://doi.org/10.1371/journal.pgen.1010650.g003

mutants (p = 0.0731) (Fig 4E and 4F). These data suggest that PAPP-AA may be required to suppress dopamine signaling, and are consistent with a scenario in which dopaminergic inhibition somewhat normalizes behavioral deficits in *pappaa* mutants.

Finally, we performed whole-brain activity mapping in *pappaa* mutant animals. Upon analyzing the resultant MAP-maps, we observed a subtle downregulation of neuronal activity particularly in the hindbrain, as well as upregulation of activity particularly in the olfactory bulb, pallium, subpallium, preoptic area, and hypothalamus (Fig 4G–4I). These activity patterns are inverted when compared to those obtained by treatment of wild type animals with the dopamine antagonist Butaclamol. Specifically, in Butaclamol-treated animals, activity in the hindbrain is increased and activity is decreased within the olfactory bulb, pallium, subpallium, preoptic area, and hypothalamus. These opposing activity signatures in *pappaa* mutants and dopamine-inhibited animals, together with the finding that Butaclamol restores habituation learning in *pappaa* mutants, are consistent with a scenario in which PAPP-AA regulates habituation learning by limiting endogenous dopamine signaling.

CACNA2D3 acts independently of other regulators of habituation learning

We recently identified the *calcium channel voltage dependent alpha2/delta subunit 3* gene, *cacna2d3*, encoding an auxiliary subunit of the voltage-gated calcium channel (VGCC) complex, as a genetic regulator of habituation learning [29]. We wondered how this VGCC subunit cooperates with the other regulators of habituation learning and therefore repeated our pharmacogenetic screen in the *cacna2d3* mutant background. We found that like *pappaa* and *kcna1a*, treatment of *cacna2d3* mutants with either the NMDA inhibitor MK801 or the glycinergic signaling inhibitor Strychnine further reduced habituation learning when compared to DMSO treated *cacna2d3* mutants (Fig 5A–5D), consistent with a model in which *cacna2d3* regulates habituation independently of NMDA and glycinergic signaling. We next examined the interaction between *cacna2d3* and dopamine signaling (Fig 5E). Analysis of the learning curves for this experiment revealed an almost flat learning curve for Butaclamol-treated siblings and mutants (Fig 5F), consistent with a strong effect of dopaminergic inhibition on habituation in *cacna2d3* mutants, and consistent with a model in which dopamine and *cacna2d3* function in parallel to regulate habituation learning. Although this effect failed to reach statistical significance, the impacts of MK801, Strychnine, and Butaclamol on *cacna2d3* mutant learning curves suggest that *cacna2d3* functions independently from NMDA, glycine, and dopamine signaling.

When we performed whole-brain imaging in *cacna2d3* mutants, we observed inconsistent activity changes across all stimulus conditions (Fig 5G–5I). This lack of a defined whole-brain activity signature is unique to *cacna2d3* among the three pharmacological and five genetic manipulations that we tested. We interpret these results to reflect that CACNA2D3 may induce only subtle changes in neuronal activity or that it may simultaneously upregulate and downregulate activity within physically commingled neuronal populations.

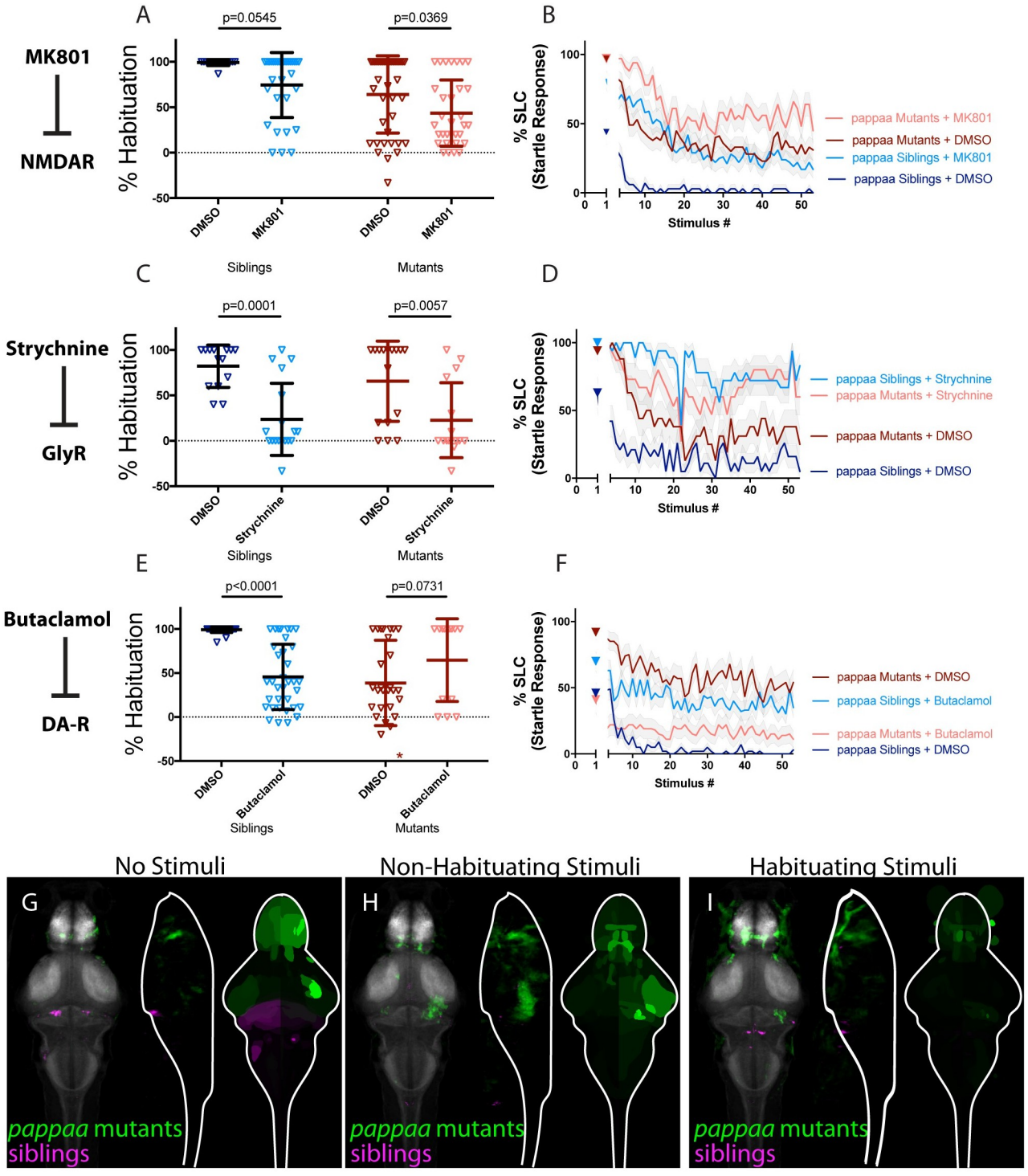

Fig 4. PAPP-AA promotes habituation by limiting endogenous dopamine signaling. (A-B) MK-801 significantly enhances habituation learning deficits observed in *pappaa* mutant larvae, indicating that NMDA signaling and *pappaa* may act within parallel molecular or circuit pathways to regulate habituation learning (p = 0.0369, n = 39 DMSO-mutants, n = 32 MK-801 mutants; p = 0.0545, n = 16 DMSO-siblings, n = 31 MK-801 siblings; p = 0.7637 indicates non-significant interaction between drug treatment and genotype). **(C-D)** Strychnine significantly enhances habituation learning deficits observed in *pappaa* mutant larvae, indicating that glycine signaling and *pappaa* may act within parallel molecular or circuit pathways to regulate habituation learning (p = 0.0057, n = 16 DMSO-mutants, n = 15 Strychnine-mutants; p = 0.0001, n = 14 DMSO-Siblings, n = 18 Strychnine-siblings; p = 0.4286 indicates non-significant interaction between drug treatment and genotype). **(E-F)** Butaclamol does not significantly enhance habituation learning deficits observed in *pappaa* mutant larvae, but rather trends toward significantly restoring habituation learning (p<0.0001, n = 31 DMSO-

siblings, n = 35 Butaclamol-siblings; p = 0.0731, n = 28 DMSO mutants, n = 13 Butaclamol mutants; p<0.0001 indicates significant interaction between drug treatment and genotype). *indicates a mutant+DMSO individual with % hab value below y-axis limit at -100% **(G-I)** Regions upregulated in *pappaa* mutants are indicated in green; regions downregulated in *pappaa* mutants are indicated in magenta. In all images, the left panel is a summed z-projection of the whole-brain activity changes. The middle panel is a summed x-projection of the whole brain activity changes. The right panel is a z-projection of the analyzed MAP-map. Patterns of neuronal activity are similar between "no stimuli" vs "non-habituating stimuli" vs. "habituating stimuli" (increased activity within the telencephalon and hypothalamus; decreased activity within multiple rhombencephalic loci). This pattern is somewhat inverted relative to that observed in Butaclamol-treated animals, consistent with a role for *pappaa* in regulating dopamine signaling. See also S1–S3 Tables for ROIs up- and down-regulated in each condition, as well as in independent replicates.

https://doi.org/10.1371/journal.pgen.1010650.g004

AP2S1 promotes habituation by limiting endogenous dopamine signaling

We recently identified a splice site mutation in the *adaptor related protein complex 2 subunit sigma 1* (*ap2s1*) gene, positioning the AP-2 adaptor complex as a fifth genetic regulator of habituation learning. We previously demonstrated that besides its role in habituation learning, AP-2 modulates sensorimotor decision-making via the Calcium-Sensing Receptor, CaSR [27,33]. Yet whether AP-2 also modulates NMDA, dopamine, or glycinergic signaling to regulate habituation learning has not been examined. We therefore performed our reduced-intensity habituation assay in *ap2s1* mutants and siblings and found that NMDA-receptor inhibition by MK-801 significantly impaired habituation in *ap2s1* mutants, indicating that these two regulators of learning function in parallel (Fig 6A and 6B). Although not statistically significant (p = 0.0773), glycinergic inhibition in the context of *ap2s1* mutations also revealed a clear and dramatic trend toward enhancement of habituation learning deficits (Fig 6C and 6D). Finally, while Butaclamol-mediated inhibition of dopamine signaling led to significantly impaired habituation in *ap2s1* siblings, Butaclamol treatment of *ap2s1* mutants significantly restored learning (p = 0.0206; Fig 6E and 6F).

Finally, we performed whole-brain activity mapping in *ap2s1* mutants. Given that inhibition of dopamine partially restored habituation in both *pappaa* and *ap2s1* mutants, we predicted that *ap2s1* mutants would exhibit a similar activity pattern to that observed in *pappaa* mutants, and an inverted pattern with respect to dopamine receptor-inhibited animals. Indeed, analysis of whole-brain activity maps in *ap2s1* mutants revealed activity patterns similar to those we observed in *pappaa* mutants (Fig 6G–6I), characterized by a marked downregulation in areas of the hindbrain that were observed to be upregulated in Butaclamol-treated animals, including a small hindbrain cluster of Tyrosine Hydroxylase (th, the enzyme required for dopamine synthesis) positive neurons (S1 Table). Moreover, significant upregulation of activity was observed in the olfactory bulb, subpallium, pallium, and intermediate hypothalamus, all areas that saw significant upregulation in *pappaa* mutant brains and downregulation in Butaclamol-treated animals (S1 Table). Combined, these results suggest a model in which AP2S1, like PAPP-AA, suppresses dopamine signaling. As in the case of *pappaa*, loss of *ap2s1* results in dysregulated dopaminergic signaling that can be restored through its pharmacological inhibition via Butaclamol.

In summary, comparing pharmacogenetic analyses and brain activity signatures across five different habituation genes and three inhibitors of habituation-regulatory neurotransmitter pathways reveals distinct molecular modules that regulate habituation learning and identifies molecularly defined brain regions associated with each of the modules.

ap2s1 and *pappaa* regulate activity in brain regions enriched for Tyrosine Hydroxylase expression

To further examine the relationship between *pappaa*, *ap2s1*, and dopamine signaling, we overlaid the Z-brain-registered tyrosine hydroxylase (Th) stain [31] with our *ap2s1* and *pappaa*

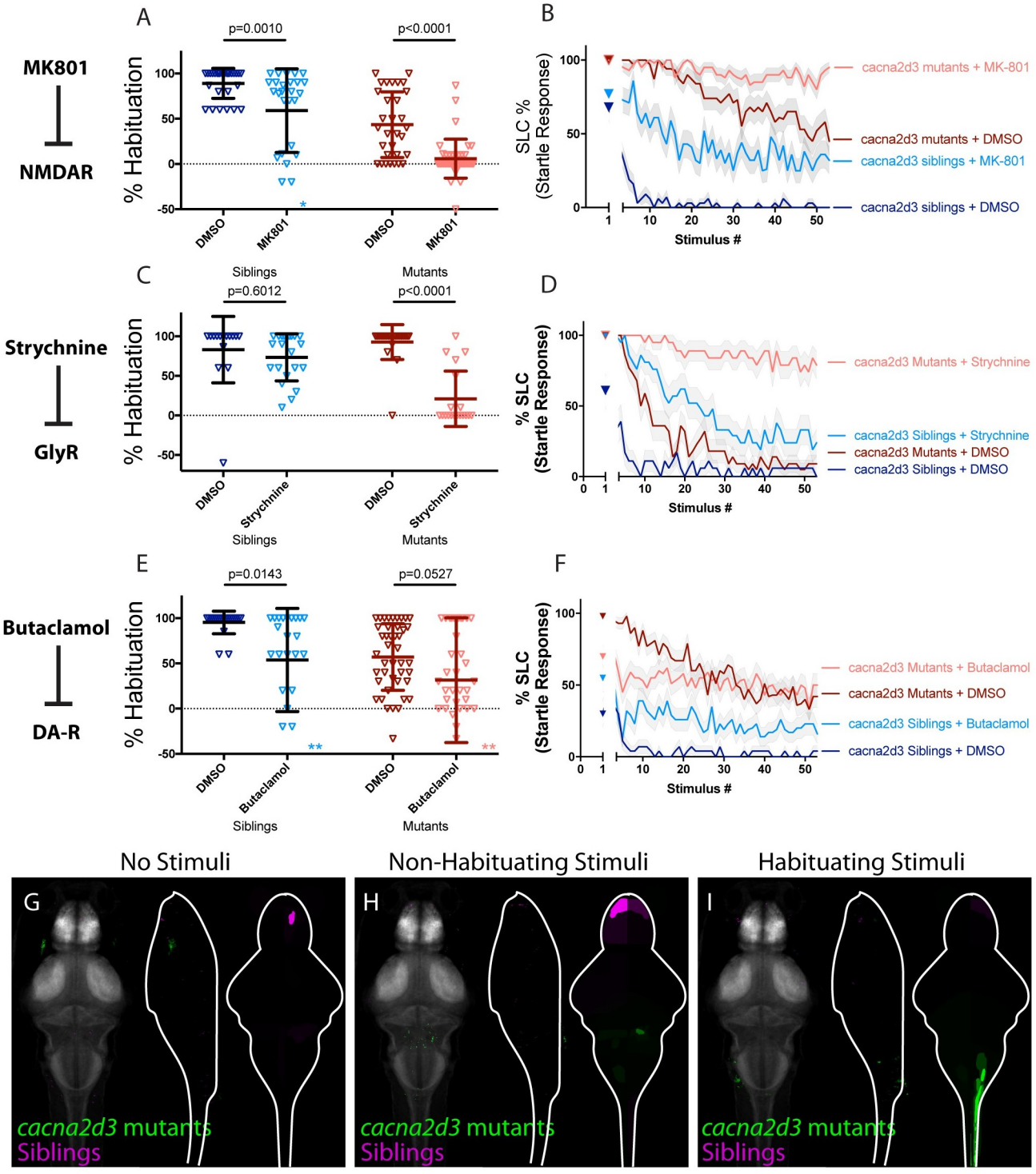

Fig 5. CACNA2D3 acts independently of other regulators of habituation learning. (A-B) MK-801 significantly enhances habituation learning deficits observed in *cacna2d3* mutant larvae, indicating that NMDA signaling and *cacna2d3* may act within parallel molecular or circuit pathways to regulate habituation learning ($p = 0.0010$, n = 28 DMSO siblings, n = 27 MK-801 siblings, vs. $p<0.0001$, n = 31 DMSO mutants, n = 41 MK-801 mutants; $p = 0.5130$ indicates non-significant interaction between drug treatment and genotype). *indicates a sibling+MK801 individual with a % hab value below y-axis limit at -60% **(C-D)** Strychnine significantly enhances habituation learning deficits observed in *cacna2d3* mutant larvae, indicating that glycine signaling and *cacna2d3* may act within parallel molecular or circuit pathways to regulate habituation ($p = 0.6012$, n = 15 DMSO siblings, n = 21 Strychnine siblings vs. $p<0.0001$, n = 22 DMSO mutants, n = 19 Strychnine mutants; $p<0.0001$ indicates significant interaction between drug treatment and genotype owing to minimal reaction of *cacna2d3* siblings to Strychnine treatment). **(E-F)** Butaclamol does not significantly enhance habituation

learning deficits observed in *cacna2d3* mutant larvae (p = 0.0143, n = 20 DMSO siblings, n = 24 Butaclamol siblings, vs. p = 0.0527, n = 43 DMSO mutants, n = 35 Butaclamol mutants; p = 0.4035 indicates non-significant interaction between drug treatment and genotype). Inspection of the learning curves **(F)** reveals a dramatic difference in the learning curves of mutants with or without drug. *indicate 2 sibling+Butaclamol and 2 mutant+Butaclamol individuals with % hab value below y-axis limit at -100%, -60%, -256%, and -80% respectively. **(G-I)** Regions upregulated in *cacna2d3* mutants are indicated in green; regions downregulated in *cacna2d3* mutants are indicated in magenta. In all images, the left panel is a summed z-projection of the whole-brain activity changes. The middle panel is a summed x-projection of the whole brain activity changes. The right panel is a z-projection of the analyzed MAP-map. Unlike other mutants, *cacna2d3* mutants do not exhibit reproducible changes in neuronal activity relative to their siblings in any stimulation condition. See also S1–S3 Tables for ROIs up- and down-regulated in each condition, as well as in independent replicates.

https://doi.org/10.1371/journal.pgen.1010650.g005

MAP-maps. Tyrosine hydroxylase is required for dopamine synthesis and therefore is expected to label dopamine neurons. Consistent with our hypothesis that *ap2s1* and *pappaa* suppress endogenous dopamine signaling, we found that activity within Th-stained olfactory bulb neurons was significantly upregulated in *ap2s1* mutants, while activity within Th-stained preoptic neurons was significantly upregulated in *pappaa* mutants. To further examine this relationship, we conducted additional independent replicates of our MAP-mapping experiments examining whole-brain activity differences in mutants relative to siblings in response to habituating stimuli. In total, our 6 *ap2s1* MAP-maps generated using habituating stimuli consistently identified "Olfactory Bulb Dopaminergic Neuron Area" as the top upregulated region in every replicate. When we overlaid the registered anti-Th stain with our *ap2s1* MAP-maps, we found that the upregulated regions indeed consistently included areas that stained positively for tyrosine hydroxylase (Fig 7A–7B"). In contrast, the *pappaa* replicates showed substantial variability in the pattern of olfactory bulb dopaminergic neuron upregulation (Fig 7C–7D'). Despite this variability, the most consistently upregulated region (upregulated in all 7 replicates) for *pappaa* was the "Preoptic otpb cluster." When we overlaid our MAP-maps with the anti-Th stain, we found that this area indeed stains positively for tyrosine hydroxylase (Fig 7E–7F"). Conversely, *ap2s1* mutants did not show increased activity within these populations (Fig 7G–7H').

To further quantify these activity changes, we measured the ratio of phosphorylated ERK to total Erk within ROIs drawn individually around left and right olfactory bulb dopamine neuron clusters as well as left and right preoptic area dopamine clusters. We then calculated a fold change in activity for our mutants relative to their siblings within each ROI. Consistent with our MAP-maps, activity within the olfactory bulb dopaminergic neurons was upregulated in both *ap2s1* and *pappaa* mutants, while activity within the preoptic dopaminergic neurons was upregulated only in *pappaa* mutant animals (Fig 7I and 7J). To examine the consistency of our findings across replicates, we computed a fold change within each ROI for all of the mutants relative to the sibling average comprising each replicate and plotted these values (Fig 7K and 7L). Taken together, these data support our hypothesis that *pappaa* and *ap2s1* act to suppress endogenous dopamine signaling. Finally, both the olfactory bulb and the preoptic area have previously been shown to increase their activity in response to acoustic stimuli, whereas activity returns toward baseline in response to habituating stimuli [34]. Therefore, we hypothesize that the hyperactivation of these same areas including during habituation in our mutants indicates dysregulation of candidate habituation-relevant brain areas. Our data do not allow us to rule out potential involvement of other candidate regions. Similarly, it is possible that *ap2s1* and/or *pappaa* may additionally exert their effects through the regulation of dopamine receptor signaling rather than through modulating of the activity of dopaminergic populations.

Discussion

We set out to map genetic regulators onto the circuit / neurotransmitter systems that drive habituation learning. We employed two complementary strategies. First, we modified the

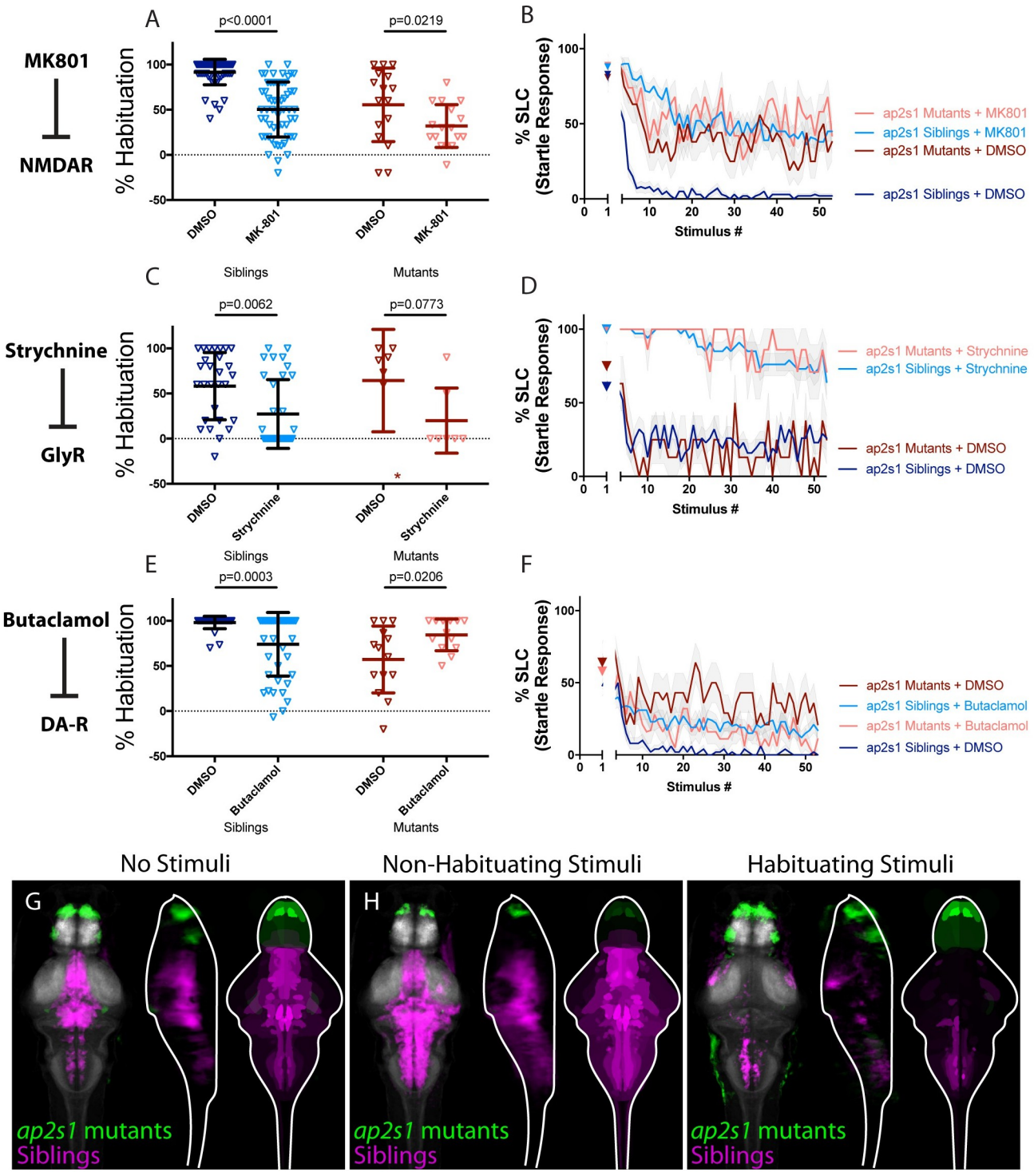

Fig 6. AP2S1 promotes habituation by limiting endogenous dopamine signaling. (A-B) MK-801 significantly enhances habituation learning deficits observed in *ap2s1* mutant larvae, indicating that NMDA signaling and *ap2s1* may act within parallel molecular or circuit pathways to regulate habituation ($p<0.0001$, n = 54 DMSO Siblings, n = 58 MK-801 siblings; $p = 0.0219$, n = 16 DMSO mutants, n = 17 MK-801 mutants; $p = 0.0875$ indicates non-significant interaction between drug treatment and genotype). **(C-D)** Strychnine trends toward enhancing habituation learning deficits observed in *ap2s1* mutant larvae ($p = 0.0062$, n = 29 DMSO siblings, n = 33 Strychnine siblings; $p = 0.0773$, n = 7 DMSO mutants, n = 7 Strychnine mutants; $p = 0.5651$ indicates non-significant interaction between drug treatment and genotype). Inspection of learning curves in **(D)** shows dramatic differences between vehicle and drug-treated larvae, indicating that glycine signaling and *ap2s1* act within parallel molecular or circuit pathways to regulate habituation learning. *indicates a mutant+DMSO individual with a % hab value below y-axis limit at -60% **(E-F)** While Butaclamol inhibits habituation learning in

siblings (p = 0.0003, n = 36 DMSO siblings, n = 42 Butaclamol siblings) it does not significantly enhance habituation learning deficits in *ap2s1* mutant larvae. Rather, *ap2s1* mutant animals learn significantly more robustly in the presence of the normally habituation-blocking Butaclamol (p = 0.0206, n = 14 DMSO mutants, n = 13 Butaclamol mutants; p<0.0001 indicates significant interaction between drug treatment and genotype). **(G-I)** Regions upregulated in *ap2s1* mutants are indicated in green; regions downregulated in *ap2s1* mutants are indicated in magenta. In all images, the left panel is a summed z-projection of the whole-brain activity changes. The middle panel is a summed x-projection of the whole brain activity changes. The right panel is a z-projection of the analyzed MAP-map. Consistent with the even stronger effect of Butaclamol in driving habituation learning in *ap2s1* mutants relative to *pappaa* mutants, *ap2s1* mutant animals exhibit an even more dramatically inverted pattern relative to Butaclamol-treated animals. *ap2s1* mutant animals exhibit robust upregulation in the telencephalon (while Butaclamol-treated animals show downregulation here). Similarly, *ap2s1* mutants show dramatically downregulated activity within the rhombencephalon, while our Butaclamol results indicate that dopamine inhibition upregulates activity here. See also S1–S3 Tables for ROIs up- and down-regulated in each condition, as well as in independent replicates.

https://doi.org/10.1371/journal.pgen.1010650.g006

standard habituation learning assay such that additive habituation learning deficits caused by combining genetic and pharmacological regulators of habituation can readily be detected and quantified. We reasoned that the habituation deficits caused by a given genetic mutation would be enhanced by pharmacological manipulations of independent or parallel habituation-regulatory pathways, but not by manipulation of habituation-regulatory mechanisms in the same pathway module. Importantly, the pharmacological manipulations we employed lack spatial specificity. Therefore, this approach is highly valuable for identifying interactions between pathways, but it does not pinpoint precisely where in the brain those interactions occur, i.e. whether the identified interactions between neurotransmitter signaling pathways and gene products occur within individual cells or within distinct nodes of a circuit regulating habituation learning. Importantly, this approach has been utilized in previous studies in which manipulations that increase dopaminergic signaling render animals hypo-responsive to dopamine receptor agonism [35]. Similarly, manipulations that decrease NMDA receptor localization render animals hypo-responsive to NMDA receptor antagonism [36].

Second, we performed MAP-mapping in the context of each pharmacological or genetic manipulation, resulting in a unique set of brain activity maps, all of which reflect habituation learning deficient patterns of activity. We are struck by the diversity of brain activity patterns associated with deficits in habituation learning. Although overlapping patterns were observed for *hip14*, MK-801, and Butaclamol, as well as for *pappaa* and *ap2s1*, these two putative modules differ from one another, and from the patterns observed for Strychnine and *kcna1a*, as well as from the observed lack of activity changes in *cacna2d3* mutants. Taken together, these results are consistent with at least two potential interpretations. For one, it is possible that although each perturbation broadly impacts brain activity in distinct ways, brain activity maps for regulators of learning overlap within a handful of critical regions that drive habituation. Alternatively, it is possible that habituation learning is tightly regulated and involves the cooperation of multiple parallel genetic-circuit modules. The latter interpretation is consistent with our observation that some genetic regulators of habituation learning show a significant interaction with NMDA and/or dopamine signaling, while others do not. Moreover, our proposal of the existence of parallel short-term habituation-regulatory modules mirrors the previous finding that long-term habituation learning in the larval zebrafish is regulated by multiple parallel processes [15].

Our results suggest the existence of five distinct habituation regulatory modules (Fig 8A). The first module consists of Hip14, as well as NMDA and dopamine signaling (Fig 8B). Our pharmacological screen uncovered significant pharmacogenetic interactions between *hip14* and inhibitors of both NMDA and dopamine receptor signaling. Additionally, an unbiased clustering algorithm identified that brain activity patterns produced by the NMDA inhibitor MK-801 and the dopamine receptor antagonist Butaclamol are similar, and the relative strengths of activity changes from these treatments are highly correlated (R-squared = 0.71,

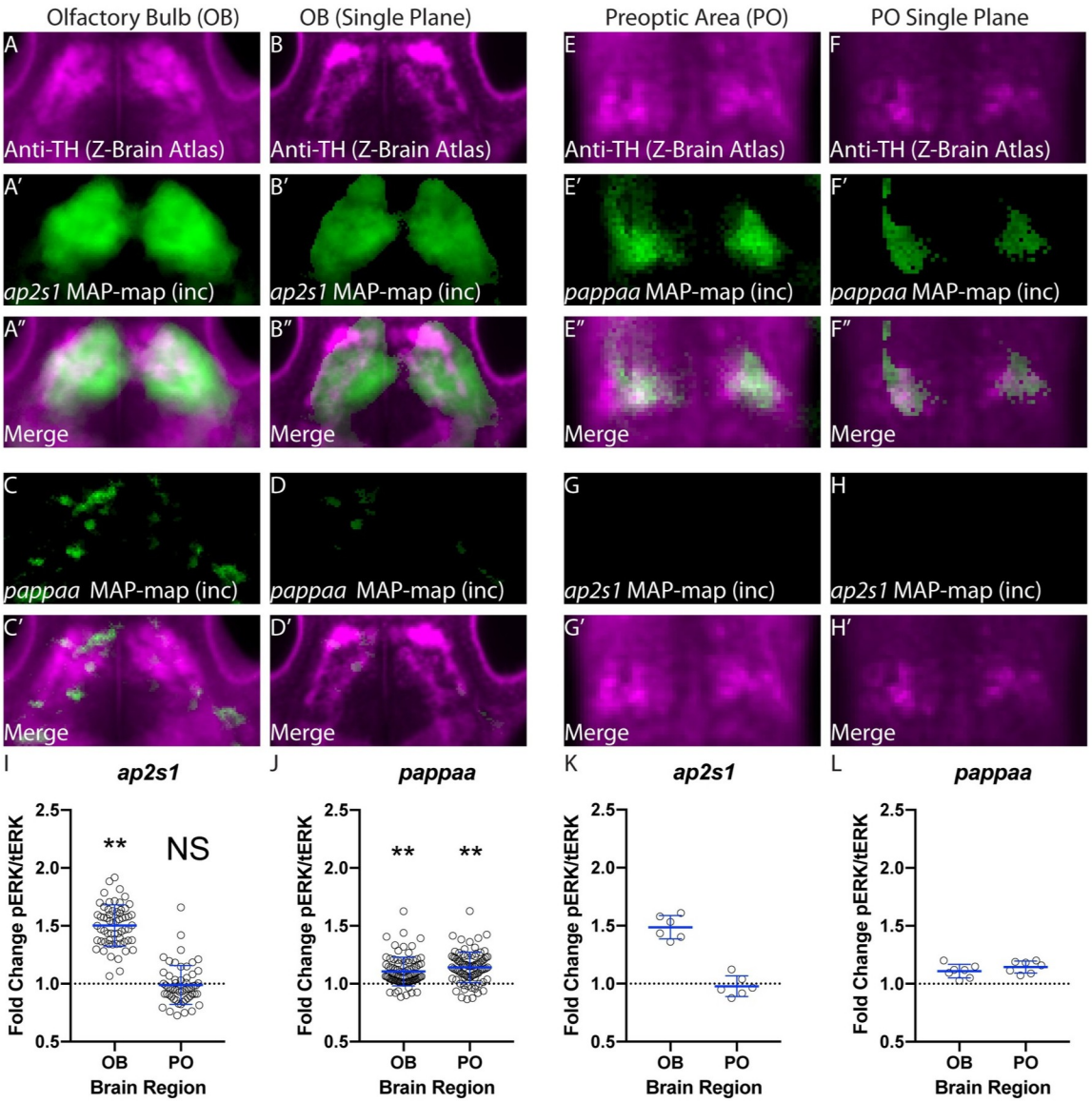

Fig 7. Th-immunoreactive neurons in the olfactory bulb and preoptic area show increased activity in *ap2s1* and *pappaa* mutants respectively. (A) Summed Z-projection of Th signal within the olfactory bulb obtained from the Z-brain Atlas [31]. (A') Representative example of a summed projection from a single experiment showing regions of increased activity within the olfactory bulb in *ap2s1* mutants relative to their siblings during habituation learning. (A") A merge of **A** and **A'** showing co-registration of Th-immunoreactive areas and regions of increased activity in *ap2s1* mutants relative to siblings during habituation. Areas of increased activity in *ap2s1* mutants during habituation learning show strong overlap with Th-immunoreactive olfactory bulb regions. **(B)** A single z-plane through the olfactory bulb Th-stained area shown in **(A). (B')** The same z-plane as in **B** taken from the stack in **A'** showing regions of increased activity within the olfactory bulb in *ap2s1* mutants relative to their siblings during habituation learning. **(B")** Merge of **(B)** and **(B')**. The x-y overlap indicated in **(A-A")** occurs within the same z-plane. **(C-C')** same as **(A'-A")** but for *pappaa* mutants. **(D-D')** same as **(B'-B)** but for *pappaa* mutants. **(E)** Summed Z-projection of anti-Th signal within a sub-region of the preoptic area obtained from the Z-brain Atlas [31]. **(E')** Representative example of a summed projection from a single experiment showing regions of increased activity within the preoptic area in *pappaa* mutants relative to their siblings during habituation learning. **(E")** A merge of **E** and **E'** showing co-registration of Th-stained areas and regions of increased activity in *pappaa* mutants relative to siblings during habituation. Areas of increased activity in *pappaa* mutants during habituation learning show strong overlap with Th-positive preoptic regions. **(F)** A single z-plane through the preoptic area shown in **(E)**. **(F')** The same z-plane as in **(F)** taken from the stack in **E'** showing regions of increased activity within the preoptic area in *pappaa* mutants relative to their siblings during habituation learning. **(F")** Merge of **(F)** and **(F')**. The x-y overlap indicated in **(E'-E")** occurs within the same z-plane. **(G-G')** same as **(E'-E")** but for *ap2s1* mutants. **(H-H')** same as (F'-F") but for *ap2s1* mutants. *ap2s1* mutants do not show upregulation within neurons of the preoptic area that stain positive for Th. **(I)** Quantification of the fold-change in pERK/tERK in *ap2s1* mutants relative to their siblings within ROIs encompassing either the olfactory bulb dopaminergic area on each side or ROIs encompassing the preoptic dopamine clusters on each side. Each point represents the region-specific fold-

change for a single larva. Larvae are pooled from all replicates. Olfactory bulb, n = 61 mutants, Wilcoxon Signed Rank Test comparing to null hypothesis of median 1 for the fold change in pERK/tERK in mutants as compared to siblings, $p<0.0001$. Preoptic area, n = 56 mutants, Wilcoxon Signed Rank Test comparing to null hypothesis of 1 for the fold change in pERK/tERK in mutants as compared to siblings, p = 0.9436. **(J)** As in **(I)** but for *pappaa* mutants relative to their siblings. Olfactory bulb n = 89 mutants. Wilcoxon Signed Rank Test comparing to null hypothesis of 1 for the fold change in pERK/tERK in mutants as compared to siblings, $p<0.0001$. Preoptic area n = 88 mutants, Wilcoxon Signed Rank Test comparing to null hypothesis of 1 for the fold change in pERK/tERK in mutants as compared to siblings, $p<0.0001$. **(K)** The same data set as in **(I)** but showing the aggregated fold-change averages within each of the 6 *ap2s1* replicates to demonstrate high degree of replicability across experiments. Each point is the pERK/tERK fold-change averaged across all animals for a single replicate. Olfactory Bulb, n = 6 replicates, Bonferroni-adjusted p = 0.0624 trends toward significance. **(L)** The same data set as in **(J)** but showing aggregated fold-change averages within each of the 7 *pappaa* replicates to demonstrate high degree of replicability across experiments. Each point is the pERK//tERK fold-change averaged across all animals for a single replicate. Olfactory bulb and preoptic area, each n = 7 replicates, Bonferroni-adjusted for both p = 0.0468. See S2 Fig for activity decreases within these same regions.

https://doi.org/10.1371/journal.pgen.1010650.g007

$p<0.05$; S3A and S3B Fig). Although both Strychnine and mutations in *hip14* broadly upregulate neuronal activity, the specific regions that they upregulate are only weakly correlated (R-squared = 0.24, $p<0.05$, S3C Fig). This finding is consistent with the results from our pharmacogenetic approach, which placed these two regulators into pathways independent of each other.

The second module consists of Hip14 and Kv1.1 (Fig 8C). Mutations in both *hip14* and *kcna1a* strongly upregulate activity in the spiral fiber neuron clusters as well as in V2a neurons

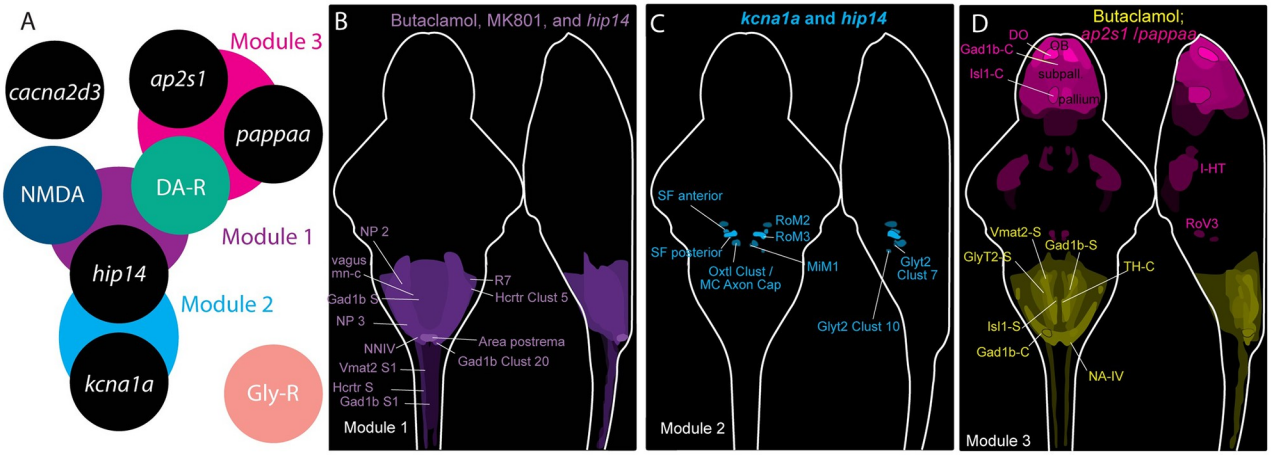

Fig 8. Cluster analysis proposes candidate habituation regulatory modules. (A) Module 1 (purple) comprises *hip14*, NMDA, and dopamine receptors. Module 2 (aqua) comprises *hip14* and *kcna1a*. Module 3 (pink) comprises *ap2s1*, *pappaa*, and dopamine receptors. Modules 4 and 5 are comprised of *cacna2d3* and glycine receptor signaling acting in parallel to all other modules. **(B)** Regions commonly upregulated by dopamine inhibition, NMDA inhibition, and mutations in *hip14* are indicated in purple. **(C)** Regions upregulated by mutations in *kcna1a* and *hip14* are indicated in blue. **(D)** Regions downregulated by dopamine receptor inhibition and upregulated by mutations in *ap2s1* or *pappaa* are indicated in pink. Regions upregulated by dopamine receptor inhibition and downregulated by mutations in *pappaa* or *ap2s1* are indicated in yellow. See also S3 Fig for cluster analysis heat map and correlations between pharmacogenetic treatments. In **(B-D)**, signal intensity is proportional to the sum of the absolute intensity values. Abbreviations in **(B)**: NP2 = Rhombencephalon–Neuropil Region 2, X vagus mn cluster = Rhombencephalon—X Vagus motorneuron cluster, Gad1b S = Rhombencephalon Gad1b Stripe 2, NP3 = Rhombencephalon Neuropil Region 3, NNIV = Rhombencephalon—Noradrendergic neurons of the Interfascicular and Vagal areas, Vmat2 S1 = Spinal Cord—Vmat2 Stripe1, Hcrtr S = Spinal Cord—6.7FDhcrtR-Gal4 Stripe, Gad1b S1 = Spinal Cord —Gad1b Stripe 1, R7 = Rhombomere 7, Hcrtr Clust 5 = Rhombencephalon—6.7FDhcrtR-Gal4 Cluster 5, Area postrema = Rhombencephalon Area Postrema, Gad1b Clust 20 = Rhombencephalon—Gad1b Cluster 20. Abbreviations in **(C)**: SF anterior = Rhombencephalon—Spiral Fiber Neuron Anterior cluster, SF posterior = Rhombencephalon—Spiral Fiber Neuron Posterior cluster, Oxtl Clust MC Axon Cap = Rhombencephalon—Oxtl Cluster 2 Near MC axon cap, RoM2 = Rhombencephalon—RoM2, RoM3 = Rhombencephalon–RoM3, MiM1 = Rhombencephalon—MiM1. Abbreviations in **(D)**: DO = Telencephalon—Olfactory bulb dopaminergic neuron areas, Gad1b-C = Telencephalon—Subpallial Gad1b cluster, Isl1-C = Telencephalon—Isl1 clusters 1 and 2, OB = Telencephalon—Olfactory Bulb, Subpall = Telencephalon–Subpallium, Pallium = Telencephalon–Pallium, Vmat2-S = Rhombencephalon—Vmat2 Stripe2, GlyT2-S = Rhombencephalon—Glyt2 Stripe 2, Isl1b-S = Rhombencephalon Isl1 Stripe1, Gad1b-C = Rhombencephalon—Gad1b Cluster 20, Gad1b-S = Rhombencephalon—Gad1b Stripe 2, TH-C = Rhombencephalon—Small cluster of TH stained neurons

https://doi.org/10.1371/journal.pgen.1010650.g008

(S3D Fig). Dysfunction of V2a neurons within the spinal cord was previously proposed as a potential mechanism underlying the kinematic deficits observed in *kcna1a* mutants [32], and we now hypothesize that hyperactivation of V2a neurons within the hindbrain could contribute to the habituation deficits observed in *kcna1a* mutants. Spiral fibers also constitute an attractive locus for Kv1.1's activity in regulating habituation. We previously showed that Hip14 can palmitoylate Kv1.1 and that it regulates its localization to the spiral fiber terminals [28]. Moreover spiral fibers are known to undergo plasticity during habituation learning [37]. Interestingly, these neurons were not reliably identified as showing differential activity in MK-801 or Butaclamol-treated animals (Module 1). One possible explanation for this is that changes within spiral fibers are below the detection threshold of our MAP-mapping analysis. Alternatively, Hip14, NMDA, and dopamine signaling could regulate habituation learning in a pathway that is parallel to the role of Hip14 and Kv1.1 within spiral fibers. This would be consistent with *hip14* mutants' stronger habituation deficit relative to *kcna1a* mutants, as well as the finding that Hip14 acts in a common pathway with dopaminergic and NMDA signaling while Kv1.1 does not.

The third module includes PAPP-AA and AP2S1 and is defined by its unique relationship to dopamine signaling. While Hip14 seems to promote dopaminergic signaling our data strongly suggest that PAPP-AA and AP2S1 oppose dopamine signaling. We first examined this relationship through overlaying the top upregulated regions with tyrosine hydroxylase stains, reasoning that if *pappaa and ap2s1* are required to downregulate endogenous dopamine signaling, then these populations may be upregulated in mutants (Fig 7). Next we used MAP-mapping to identify regions whose activity is oppositely regulated by Butaclamol and *ap2s1*/*pappaa*. This revealed that activity is broadly upregulated in the telencephalon in *ap2s1* mutants and in *pappaa* mutants, and downregulated in the telencephalon by Butaclamol treatment. Similarly, activity in the hindbrain is largely upregulated by Butaclamol treatment and downregulated in *ap2s1* mutants (Fig 8D, S3E and S3F Fig). We hypothesize that the opposing function of D1 and D2/D3-type dopamine receptors in regulating the startle response may help to explain the surprising bi-directional control of habituation learning by dopamine signaling [38]. While dopamine acts to drive habituation learning (reducing stimulus responsiveness) through D1-type dopamine receptors, it is known that it additionally promotes stimulus responsiveness through D2/D3-type dopamine receptors in mice [38]. We propose that AP2S1 and PAPP-AA are required to limit signaling through D2/D3-type dopamine receptors. In this scenario, mutations in either gene would result in excessive D2/D3 signaling and hyperresponsive larvae that fail to habituate to acoustic stimuli. Under these conditions, applying a dopamine receptor antagonist might normalize D2/D3 signaling and stimulus responsiveness, allowing animals to habituate. In support of this, work in zebrafish has shown that high doses of the D2 receptor antagonist amisulpride can promote habituation learning [39], and that the D2 antagonist haloperidol promotes long-term habituation of the O-bend or visual startle [15].

The whole brain activity patterns observed for AP2S1 resemble the brain activity maps recently published for low-habituating populations obtained through breeding selection, showing increased neuronal activity in the telencephalon and decreased activity in the hindbrain [34]. Moreover, our data suggest that dopaminergic neuromodulation is an important driver of activity in the larval telencephalon and are supported by recent optogenetic experiments performed in Th2-expressing neurons [40]. However, this previous work found that ablating dopaminergic neurons did not alter habituation and that dopamine neuron activity in the caudal hypothalamus was actually elevated in high-habituating populations relative to low [34]. Nonetheless, chemogenetic ablation was restricted to Th1-positive dopamine neurons whereas our pharmacological approach is expected to impact the targets of both Th1 and

Th2-expressing neurons. Moreover, the ablation approach is chronic, in contrast to our transient pharmacological inhibition, eliminating dopaminergic neurons while potentially having no immediate effect on neurotransmitter levels [41]. Given these differences, it is perhaps not surprising that these approaches yield somewhat differing results. Indeed, our opposing results underscore the complex roles that dopamine plays in regulating acoustic startle sensitivity and habituation, and further work will be required to understand the role of dopamine in regulating habituation learning.

Finally, our work is consistent with glycine signaling (Module 4) and *cacna2d3* (Module 5) functioning in parallel to one another and to the other three modules described. We find no evidence that *cacna2d3* acts to regulate dopaminergic, glycinergic, or NMDA signaling, and likewise find no pharmacogenetic interactions between Strychnine and *hip14*, *kcna1a*, *pappaa*, or *ap2s1*. Although it is possible that we failed to detect a weak interaction between these and the other modules, it will be important to investigate potential interactions between these pathways and other pharmacogenetic regulators of habituation learning. Future studies might examine these cases where our work failed to detect interactions by merging our two approaches. For example, one might examine the interactions between pharmacological and genetic regulators of habituation learning using whole-brain or Calcium imaging analyses. We predict that such studies might uncover a blunted impact of the pharmacological manipulations on neuronal activity in mutants that occupy the same functional module.

One striking and unexpected finding that arose from our data is that each pharmacological manipulation or genetic mutation induced a brain activity pattern that was remarkably consistent across stimulation conditions (S3A Fig). This is consistent with previously published work examining whole-brain activity changes in animals selectively bred for high versus low habituation rates [34]. Moreover, our data are consistent with a model in which our pharmacogenetic perturbations lead to broad impacts on brain activity. Finally, these data are consistent with the reported hypersensitivity of all of the tested mutants to low-intensity stimuli [25,28,29,33], which suggest baseline deficits in the thresholding of acoustic stimuli. Importantly, although habituation deficits may co-occur with changes in response thresholds as they do in these mutants, these deficits may also occur independently [25,42], suggesting that they are mechanistically separable. It is also possible that the similarities between MAP-maps across stimulus conditions indicate that our genetic and pharmacological manipulations impact the animals' internal state, resulting in baseline brain activity changes that manifest at the behavioral level as habituation deficits. Nonetheless, these findings are highly relevant for human health, where disorders that impact habituation learning often have simultaneous impacts on response thresholds. Taken together our results support a model in which multiple circuit mechanisms regulated by parallel molecular-genetic pathways cooperate to drive habituation learning *in vivo*.

Materials and methods

Ethics statement

All animal protocols were approved by the University of Pennsylvania Institutional Animal Care and Use Committee (IACUC).

Experimental model and subject details

hip14^{p174}, *pappaa*^{p170}, *cacna2d3*^{sa16189}, and *ap2s1*^{p172} mutants were maintained in the TLF background. *kcna1a*^{p410} was maintained in the WIK background. Among these, *cacna2d3*^{sa16189} is homozygous viable, and crosses were performed between heterozygous carriers and homozygous mutants to obtain clutches of 50% heterozygous, and 50% homozygous

mutant offspring. All other crosses were established between heterozygous carriers. Groups labeled as "mutants" are comprised of homozygous mutants, while groups labeled as "siblings" are a mix of WT and heterozygous individuals.

Pharmacogenetic behavior testing was performed in two independent runs on day 5 animals as previously described [7]. Data from these independent runs was pooled for analysis. Stimulation and fixation for MAP-mapping analysis was performed on day 6 to standardize with the reference brain utilized for registration, as previously described [31].

To ensure approximately equal numbers of mutants and siblings (siblings are a mix of heterozygous and WT animals), clutches were enriched for mutant animals prior to behavior testing or MAP-mapping by selecting for animals based on the exaggerated spontaneous movement phenotype (*kcna1a*^{p410}) or swim bladder defects (*pappaa*^{p170}, *hip14*^{p174}). To enrich for mutant animals in the absence of such phenotypes, *ap2s1* clutches were subjected to live genotyping on Day 3 as previously described [43]. After genotyping, mutant and sibling animals were mixed together in 10cm petri dishes and tested on Day 5 (pharmacogenetic behavior analysis) or stimulated and fixed on Day 6 (MAP-mapping).

For all experiments, behavior was performed and analyzed blind to genotype; genotyping was performed after behavior testing and/or imaging, and mutant animals were compared to siblings from the same clutches. Except in the case of *ap2s1* live pre-genotyping, all genotyping was performed by extracting gDNA from each larva individually through incubation in 15ul of 25mM NaOH, 0.2mM EDTA for 15 minutes at 95 degrees C. Following incubation, an equal volume (15ul) of neutralization solution (40mM Tris-HCl, pH 5) was applied to each well. 1-5ul of this mixture was then used directly for PCR or KASP genotyping.

Pharmacogenetic behavior testing

A 200x (100mM) stock of MK-801 (Sigma M107) was prepared by dissolving a new vial of 25mg of MK-801 powder in 750ul of 100% DMSO. The stock solution was then further dissolved in E3 to a final concentration of 500uM (0.5% DMSO final concentration). MK-801 was applied to a 10cm petri dish containing n = 45 5 dpf larvae 30 minutes prior to the first presentation of baseline acoustic stimuli. Control larvae received 0.5% DMSO in E3. The 200x stock of MK-801 was freeze-thawed a maximum of one time and then disposed of.

A 200x (10mM) stock of Strychnine (Sigma S0532) was prepared by dissolving 33.4mg of Strychnine powder in 10mL of 100% DMSO. The stock solution was then further dissolved in E3 to a final concentration of 50uM (0.5% DMSO final concentration). Strychnine was applied to a 10cm petri dish containing n = 45 5 dpf larvae 15 minutes prior to the first presentation of baseline acoustic stimuli. Control larvae received 0.5% DMSO in E3. The 200x stock of Strychnine was frozen at -20. We observed no reduction in the effectiveness of our Strychnine stock solution on WT animals over the course of several months of testing.

A 630x (63mM) stock of Butaclamol (Sigma D033) was prepared by dissolving 25mg of Butaclamol in 1mL of DMSO. The stock solution was further dissolved in E3, and DMSO supplemented to a final concentration of 0.5% DMSO, 100uM Butaclamol. Butaclamol was applied to a 10cm petri dish containing n = 45 5dpf larvae 30 minutes prior to the presentation of baseline acoustic stimuli. Control larvae received 0.5% DMSO in E3. The 630x stock of Butaclamol was freeze-thawed a maximum of one time and then disposed of.

The stimulus level for our behavioral experiments was chosen to allow for both increases and decreases in habituation in our mutant conditions. However we also see a higher degree of variability between experiments using this stimulus level. Therefore, each experiment is internally controlled (mutants and siblings were tested in the same dish) and replicated twice.

All larvae were acclimated to testing room conditions (light, temperature, etc.) for 30 minutes prior to the application of pharmacological agents. Assays for habituation of the acoustic startle response (ASR) were performed on 5 dpf larvae arrayed in a 36-well dish, fabricated by laser-cutting a 6x6 grid of holes into an acrylic sheet, and affixing it to an uncut sheet of the same dimensions using acrylic glue. The dish was mounted on a vibrational exciter (4810; Brüel and Kjaer, Norcross, GA) via an aluminum rod. Acoustic stimuli (2ms duration, 1000Hz waveforms) were delivered during the baseline phase of the assay with an interstimulus interval (ISI) of 40 seconds. During the habituation phase, stimuli were presented with a 3-second ISI.

MAP-mapping

Larvae were acclimated to testing room conditions (light, temperature, etc.) in a 10cm petri dish with n = 45 6 dpf larvae for 30 minutes prior to transfer to the testing arena. Following acclimation, 25 larvae were transferred from the petri dish to a cell strainer with 40um pores (Neta Scientific 431750) nested inside a 6cm petri dish, submerged in E3. The entire cell strainer was then removed and immediately submerged in a 4cm petri dish glued to a circular acrylic base, affixed via a titanium arm to the vibrational exciter (4810; Brüel and Kjaer, Norcross, GA). Larvae were acclimated to the testing arena for 30 minutes with no stimuli. "No Stimuli" runs then proceeded with 17 minutes of additional run time. "Non-Habituating Stimuli" runs proceeded with 10 35.1dB acoustic stimuli with a 90-second ISI, followed by 2 minutes of rest. "Habituating Stimuli" runs proceeded with 180 35.1dB acoustic stimuli with 5-second ISI followed by 2 minutes of rest. Immediately following the completion of the behavior testing protocol, the cell strainer was removed from the testing arena and dropped into a 6-well dish (VWR 10861–554) containing 4% PFA in 1x PBT (1x PBS + 0.25% TritonX100). After 2 minutes, cell strainers were transferred to a second 6-well dish containing cold 4% PFA in 1x PBS, and incubated at 4 degrees overnight. Next, the immunostaining procedure described in [31] was carried out as described with the following modifications: immediately after washing PFA, larvae were bleached for approximately 12 minutes in 1.5% hydrogen peroxide; 0.5% KOH; larvae were then washed twice (quickly) and then once for 5 minutes in PBT; larvae were then incubated in 150mM of Tris-HCl pH 9.0 for 5 minutes at room temperature, followed by 15 minutes at 70 degrees Celcius. Following immunostaining, all larvae for a single experiment were mounted in 1.5% low-melt agarose (Lonza Bioscience 50101) in a 50mm petri dish with a 30mm diameter glass bottom (Mattek P50G-1.5-30-F). Following mounting, a map was drawn noting the orientation and position of each larva, and numbering every larva. Confocal images were acquired using a 20x objective lens on a Zeiss LSM880 confocal microscope using Zen Software. The "tiles" function was used to acquire and stitch together two images of each brain (one centered on the rostral and one on the caudal portion of the head). Confocal images were named according to the larva numbers assigned in our map. Following imaging, each animal was unmounted from the agarose and placed in labeled strip tubes in accordance with their assigned number. We then extracted genomic DNA as described above and performed PCR or KASP genotyping.

Behavior analysis

Behavior videos were background subtracted by computing a max projection of the entire image series using FIJI. Max projections were then subtracted from each image within the series using FIJI. Subtracted image series were tracked using FLOTE software as previously described [7,8]. In the case of Strychnine-treated larvae, the previously described "accordion-like" shape [44] of the SLC response precluded acceptable tracking via FLOTE. Therefore,

behavioral responses were manually scored blind to genotype as SLCs or No-Response by isolating the 17ms of video following the delivery of the acoustic pulse, and scoring body bends within this interval as SLCs.

% Habituation was quantified by the following formula: [% Habituation = (1-[response frequency Stimuli 45–54] ÷ [response frequency baseline])*100].

Quantification and statistical analysis

Computation of means, SD, SE, and data set normality were performed using GraphPad Prism. Effects of each drug condition were assessed using Two-Way ANOVA with Sidak's Multiple Comparisons Test.

For MAP-mapping, image registration and positive and negative significant delta median signals in each brain region across mutant vs. sibling and drug vs. DMSO controls were calculated using the standard MAP-mapping pipeline as described in [31].

For ROI-specific computation of pERK/tERK, we used the ROIbasedpERKanalysis script described in [45]. Using this script, we first specified two sets of ROIs used across all of our samples, one encompassing the Th-immunoreactive signal within the preoptic otpb clusters on the left and right side respectively, and a second set encompassing the Th-immunoreactive signal within the olfactory bulb on the left and right sides. The script computed pERK/tERK values across all of our samples within each ROI. Sibling averages were computed within each ROI and within each replicate. Fold change in each mutant was then computed for each ROI as a ratio of mutant pERK/tERK over the sibling average pERK/tERK. Data were then aggregated across all replicates. Finally, Wilcoxon signed-rank tests were used to compare mutant fold changes to a null hypothesis of a median 1 (no change relative to the siblings).

For cluster analysis, positive and negative significant delta median signals were imported into R [46,47]. Signal for each experimental replicate was normalized according to the highest absolute value in that condition, such that the highest magnitude signal for each condition was either -1 or 1. Distances were calculated using the Canberra method, which disregards data when both conditions have a value of 0; this prevented overestimation of similarity between conditions in which many brain regions had zero signal. The factoextra package [48] was used to visualize distances and clusters.

For pairwise plots, normalized negative signal in a given brain region was subtracted from normalized positive signal to obtain a single signal value for that region. We then averaged signal values for each condition (either drug or mutant allele) over all replicate data sets and behavioral stimulation paradigms. After confirming via cluster analysis that these average values captured the general patterns of similarity observed among individual replicates, we then plotted pairwise comparisons between conditions. Module maps (Fig 8B–8D) were created using a modified version of the ZBrainAnalysisOfMAPMaps function [31]. Colors were adjusted in Adobe Illustrator.

Supporting information

S1 Fig. Pharmacological inhibitors of habituation learning induce distinct patterns of brain activity changes. (A-C) Regions upregulated by the specified drug treatment under "No Stimulus" conditions are indicated in green; regions downregulated are indicated in magenta. **(D-F)** Regions upregulated by the specified drug treatment under "Non-Habituating Stimuli" conditions are indicated in green; regions downregulated are indicated in magenta. In all images, the left panel is a summed z-projection of the whole-brain activity changes. The middle panel is a summed x-projection of the whole brain activity changes. The right panel is a

z-projection of the analyzed MAP-map. Molecular targets of pharmacological agents are indicated with diagrams above each column. Note that the patterns of neuronal activity induced by a given pharmacological agent are relatively consistent across stimulation condition (i.e. "no stimuli", vs. "non-habituation stimuli", vs "habituating stimuli" in Fig 1K–1M). Moreover, although all pharmacological agents reduce habituation learning, patterns of neuronal activity are highly dissimilar between individual pharmacological treatments.
(TIF)

S2 Fig. MAP-map analysis of activity decreases within olfactory bulb and preoptic dopaminergic regions. (A-D') Regions with reduced activity in mutants relative to siblings are indicated in magenta. These signals are merged with the Z-brain-registered Th stain in green showing olfactory bulb dopaminergic neurons in figures **A-B'** and preoptic dopaminergic neurons **C-D'**. Fig 7 shows increased activity in olfactory bulb dopaminergic neurons in *ap2s1* and *pappaa* mutants and preoptic dopaminergic neurons in *pappaa* mutants. Here we show that these same regions are largely devoid of pixels showing reduced activity in mutants relative to siblings according to our MAP-maps. No areas of reduced activity are identified, except medially, outside the Th-stained area of the olfactory bulb in **A-A'**. These data are consistent with *ap2s1* and *pappaa* upregulating rather than downregulating dopamine neuron activity within these brain areas.
(TIF)

S3 Fig. Cluster analysis identifies regions of interest. (A) Heat map indicating replicability across stimulus conditions for each mutant and drug condition. Column and row labels indicate genotype or drug treatment and stimulus condition (i.e. No Stimuli = NoStim, Non-Habituating Stimuli = Taps, Hab = Habituating Stimuli). Note an intermingled cluster containing Butaclamol and MK-801. **(B-F)** Plots of pairwise comparisons between drugs and or genotypes. Color legend in **(B)** applies to all. R-square values are indicated when $p<0.05$. **(B)** Plot indicating positive correlation between MK-801 and Butaclamol signal changes. **(C)** Plot indicating a weak positive correlation between *hip14* and Strychnine signal changes. **(D)** Plot showing correlated changes in the rhombencephalon between *hip14* and *kcna1a*. **(E)** Plot showing 3 populations in Butaclamol vs. *ap2s1* changes. Largely telencephalic regions, upregulated in *ap2s1* mutants and downregulated by Butaclamol; largely rhombencephalic regions, upregulated by Butaclamol and downregulated in *ap2s1* mutants; and a large number of regions downregulated by both manipulations. **(F)** Plot showing signal changes in *pappaa* as compared to Butaclamol. Multiple telencephalic as well as diencephalic regions to a lesser degree, are anti-correlated (up-regulated in *pappaa* mutants but downregulated in Butaclamol). Brain region abbreviations in **(B)**: s1181t = Telencephalon—S1181t Cluster, Gang LLN SO2 = Ganglia—Lateral Line Neuromast SO2, Gang LLN D1 = Ganglia—Lateral Line Neuromast D1, Noradren Interfasc Vagal = Rhombencephalon—Noradrendergic neurons of the Interfascicular and Vagal areas. Brain region abbreviations in **(C)**: Lat Retic Nuc = Rhombencephalon—Lateral Reticular Nucleus. Brain region abbreviations in **(D)**: Spiral Fib Post and Ant = Rhombencephalon—Spiral Fiber Neuron Posterior and Anterior clusters, Mauth Axon Cap = Rhombencephalon—Mauthner Cell Axon Cap. Brain region abbreviations in **(E)**: DO = Telencephalon—Olfactory bulb dopaminergic neuron areas, OB = Telencephalon—Olfactory Bulb, Subpall Gad1b = Telencephalon—Subpallial Gad1b cluster, Subpall = Telencephalon–Subpallium, Oxtl Clust 1 = Rhombencephalon—Oxtl Cluster 1 Sparse, Noradren Interfasc Vagal = Rhombencephalon—Noradrendergic neurons of the Interfascicular and Vagal areas, TH-C = Rhombencephalon—Small cluster of TH stained neurons. Brain region abbreviations in **(F)**: Ant Comm = Telencephalon—Anterior Commisure, Cerebell Olig2 Enriched = Rhombencephalon—Olig2 enriched areas in cerebellum, Gang

LLN SO1 and SO2 = Ganglia—Lateral Line Neuromast SO1 and SO2.
(TIF)

S4 Fig. Analysis of kinematic parameters of acoustic startle response reveal minimal variation in drug-treated and mutant animals. Kinematic parameters for MK801, Butaclamol, *hip14*, and *pappaa* are reported (for *ap2s1*, *cacna2d2*, and *kcna1a* see references 33,29,32 respectively. Bonferroni-adjusted p-values for unpaired t-tests are reported for normally distributed data, and Bonferroni-adjusted p-values for Mann-Whitney tests are reported for data that are not normally distributed. NS = Not significant. **(A)** Butaclamol significantly increases turn duration during acoustic startle performance n = 17 Butaclamol-treated, n = 16 DMSO-treated, Bonferroni-adjusted p-value for Mann-Whitney test p = 0.044. **(B)** MK801 significantly reduces turn latency and significantly increases maximum angular velocity during acoustic startle performance. Latency: n = 20 MK801-treated, n = 21 DMSO-treated, Bonferroni-adjusted p-value for Mann-Whitney test p = 0.0004. Maximum angular velocity: n = 20 MK801-treated, n = 21 DMSO-treated, Bonferroni-adjusted p-value for Mann-Whitney test p = 0.0468. **(C)** Mutations in *hip14* significantly reduce turn latency during acoustic startle performance. n = 34 *hip14* mutants, n = 34 *hip14* siblings, Bonferroni-adjusted p-value for Mann-Whitney test p = 0.0008. **(D)** Mutations in *pappaa* significantly reduce turn latency, turn angle, and maximum angular velocity during acoustic startle performance. Latency: n = 28 *pappaa* mutants, n = 31 *pappaa* siblings, Bonferroni-adjusted p-value for Mann-Whitney test p = 0.0008. Turn Angle and maximum angular velocity: n = 28 *pappaa* mutants, n = 31 *pappaa* siblings, unpaired t-test $p<0.0001$.
(TIF)

S1 Video. Example video showing 4x looped acoustic startle responses of Strychnine-exposed animals. Annotated pink R indicates animals scored as responders. The video is looped 4x to enable better visualization of the subtle movements performed by responders.
(AVI)

S1 Table. Raw values for signal change in each ROI within each mutant and drug condition across 2–3 replicates.
(XLSX)

S2 Table. Normalized values for increased activity changes in each ROI within each mutant and drug condition across 2–3 replicates. These values were used for cluster analysis.
(XLSX)

S3 Table. Normalized values for decreased activity changes in each ROI within each mutant and drug condition across 2–3 replicates. These values were used for cluster analysis.
(XLSX)

S1 Data. Raw numbers for all graphs.
(XLSX)

S1 Code. R code used to perform cluster analysis.
(R)

Acknowledgments

The authors would like to thank the Granato lab members, as well as Dr. Owen Randlett and Dr. Roshan Jain for technical advice and feedback on our findings. The authors would also like to acknowledge Drs. Roshan Jain, Marc Wolman and Nik Santistevan for sharing *ap2s1*,

pappaa, and *cacna2d3* mutant zebrafish respectively. The authors would also like to acknowledge the Cell and Developmental Biology Microscopy Core.

Author Contributions

Conceptualization: Jessica C. Nelson, Hannah Shoenhard, Michael Granato.

Formal analysis: Jessica C. Nelson, Hannah Shoenhard.

Funding acquisition: Jessica C. Nelson, Michael Granato.

Investigation: Jessica C. Nelson.

Resources: Michael Granato.

Writing – original draft: Jessica C. Nelson.

Writing – review & editing: Jessica C. Nelson, Hannah Shoenhard, Michael Granato.

References

1. Groves PM, Thompson RF. Habituation: A dual-process theory. Psychological Review. 1970; 77: 419. https://doi.org/10.1037/h0029810 PMID: 4319167
2. Rankin CH, Abrams T, Barry RJ, Bhatnagar S, Clayton DF, Colombo J, et al. Habituation revisited: An updated and revised description of the behavioral characteristics of habituation. Neurobiology of Learning and Memory. 2009; 92: 135–138. https://doi.org/10.1016/j.nlm.2008.09.012 PMID: 18854219
3. Thompson RF, Spencer WA. Habituation: a model phenomenon for the study of neuronal substrates of behavior. Psychol Rev. 1966; 73: 16–43. https://doi.org/10.1037/h0022681 PMID: 5324565
4. Epstein LH, Temple JL, Roemmich JN, Bouton ME. Habituation as a determinant of human food intake. Psychol Rev. 2009; 116: 384–407. https://doi.org/10.1037/a0015074 PMID: 19348547
5. Kim YJ, van Rooij SJH, Ely TD, Fani N, Ressler KJ, Jovanovic T, et al. Association between posttraumatic stress disorder severity and amygdala habituation to fearful stimuli. Depress Anxiety. 2019; 36: 647–658. https://doi.org/10.1002/da.22928 PMID: 31260599
6. Pinsker H, Kuppermann I, Castellucci V, Kandel E. Habituation and dishabituation of the gill-withdrawal reflex in Aplysia. Science. 1970; 167: 1740–2. https://doi.org/10.1126/science.167.3926.1740 PMID: 5416541
7. Wolman MA, Jain RA, Liss L, Granato M. Chemical modulation of memory formation in larval zebrafish. Proceedings of the National Academy of Sciences. 2011; 108: 15468–15473. https://doi.org/10.1073/pnas.1107156108 PMID: 21876167
8. Burgess HA, Granato M. Sensorimotor gating in larval zebrafish. The Journal of Neuroscience. 2007; 27: 4984–4994. https://doi.org/10.1523/JNEUROSCI.0615-07.2007 PMID: 17475807
9. Fetcho JR, McLean DL. Startle Response. In: Squire LR, editor. Encyclopedia of Neuroscience. Oxford: Academic Press; 2009. pp. 375–379.
10. Kimmel CB, Patterson J, Kimmel RO. The development and behavioral characteristics of the startle response in the zebra fish. Developmental Psychobiology. 1974; 7: 47–60. https://doi.org/10.1002/dev.420070109 PMID: 4812270
11. Best JD, Berghmans S, Hunt JJFG, Clarke SC, Fleming A, Goldsmith P, et al. Non-associative learning in larval zebrafish. Neuropsychopharmacology. 2008; 33: 1206–1215. https://doi.org/10.1038/sj.npp.1301489 PMID: 17581529
12. Roberts AC, Reichl J, Song MY, Dearinger AD, Moridzadeh N, Lu ED, et al. Habituation of the C-start response in larval zebrafish exhibits several distinct phases and sensitivity to NMDA receptor blockade. PLoS ONE. 2011; 6: e29132. https://doi.org/10.1371/journal.pone.0029132 PMID: 22216183
13. Roberts AC, Chornak J, Alzagatiti JB, Ly DT, Bill BR, Trinkeller J, et al. Rapid habituation of a touch-induced escape response in Zebrafish (Danio rerio) Larvae. Burgess HA, editor. PLOS ONE. 2019; 14: e0214374. https://doi.org/10.1371/journal.pone.0214374 PMID: 30946762
14. Wolman M, Granato M. Behavioral genetics in larval zebrafish: learning from the young. Dev Neurobiol. 2012; 72: 366–372. https://doi.org/10.1002/dneu.20872 PMID: 22328273
15. Randlett O, Haesemeyer M, Forkin G, Shoenhard H, Schier AF, Engert F, et al. Distributed Plasticity Drives Visual Habituation Learning in Larval Zebrafish. Current biology: CB. 2019; 29: 1337–1345.e4. https://doi.org/10.1016/j.cub.2019.02.039 PMID: 30955936

16. Castro-Alamancos MA, Torres-Aleman I. Learning of the conditioned eye-blink response is impaired by an antisense insulin-like growth factor I oligonucleotide. Proc Natl Acad Sci U S A. 1994; 91: 10203–10207. https://doi.org/10.1073/pnas.91.21.10203 PMID: 7937862

17. Engel JE, Wu C-F. Altered Habituation of an Identified Escape Circuit in *Drosophila* Memory Mutants. The Journal of Neuroscience. 1996; 16: 3486–3499. https://doi.org/10.1523/JNEUROSCI.16-10-03486.1996 PMID: 8627381

18. Engel JE, Wu C-F. Genetic Dissection of Functional Contributions of Specific Potassium Channel Subunits in Habituation of an Escape Circuit in *Drosophila*. The Journal of Neuroscience. 1998; 18: 2254–2267. https://doi.org/10.1523/JNEUROSCI.18-06-02254.1998 PMID: 9482810

19. McDiarmid TA, Belmadani M, Liang J, Meili F, Mathews EA, Mullen GP, et al. Systematic phenomics analysis of autism-associated genes reveals parallel networks underlying reversible impairments in habituation. Proceedings of the National Academy of Sciences. 2020; 117: 656–667. https://doi.org/10.1073/pnas.1912049116 PMID: 31754030

20. Morrison GE, van der Kooy D. A mutation in the AMPA-type glutamate receptor, glr-1, blocks olfactory associative and nonassociative learning in Caenorhabditis elegans. Behav Neurosci. 2001; 115: 640–649. https://doi.org/10.1037//0735-7044.115.3.640 PMID: 11439453

21. Ohta A, Ujisawa T, Sonoda S, Kuhara A. Light and pheromone-sensing neurons regulates cold habituation through insulin signalling in Caenorhabditis elegans. Nat Commun. 2014; 5. https://doi.org/10.1038/ncomms5412 PMID: 25048458

22. Rankin CH, Wicks SR. Mutations of the *Caenorhabditis elegans* Brain-Specific Inorganic Phosphate Transporter *eat-4* Affect Habituation of the Tap–Withdrawal Response without Affecting the Response Itself. The Journal of Neuroscience. 2000; 20: 4337–4344. https://doi.org/10.1523/JNEUROSCI.20-11-04337.2000 PMID: 10818169

23. Swierczek NA, Giles AC, Rankin CH, Kerr RA. High-throughput behavioral analysis in C. elegans. Nature Methods. 2011; 8: 592–598. https://doi.org/10.1038/nmeth.1625 PMID: 21642964

24. Wolf FW, Eddison M, Lee S, Cho W, Heberlein U. GSK-3/Shaggy regulates olfactory habituation in Drosophila. Proceedings of the National Academy of Sciences. 2007; 104: 4653–4657. https://doi.org/10.1073/pnas.0700493104 PMID: 17360579

25. Wolman MA, Jain RA, Marsden KC, Bell H, Skinner J, Hayer KE, et al. A Genome-wide Screen Identifies PAPP-AA-Mediated IGFR Signaling as a Novel Regulator of Habituation Learning. Neuron. 2015; 85: 1200–1211. https://doi.org/10.1016/j.neuron.2015.02.025 PMID: 25754827

26. McDiarmid TA, Bernardos AC, Rankin CH. Habituation is altered in neuropsychiatric disorders-A comprehensive review with recommendations for experimental design and analysis. Neurosci Biobehav Rev. 2017; 80: 286–305. https://doi.org/10.1016/j.neubiorev.2017.05.028 PMID: 28579490

27. Jain RA, Wolman MA, Marsden KC, Nelson JC, Shoenhard H, Echeverry FA, et al. A Forward Genetic Screen in Zebrafish Identifies the G-Protein-Coupled Receptor CaSR as a Modulator of Sensorimotor Decision Making. Current Biology. 2018; 28: 1357–1369.e5. https://doi.org/10.1016/j.cub.2018.03.025 PMID: 29681477

28. Nelson JC, Witze E, Ma Z, Ciocco F, Frerotte A, Randlett O, et al. Acute Regulation of Habituation Learning via Posttranslational Palmitoylation. Current Biology. 2020; 30: 2729–2738.e4. https://doi.org/10.1016/j.cub.2020.05.016 PMID: 32502414

29. Santistevan NJ, Nelson JC, Ortiz EA, Miller AH, Halabi DK, Sippl ZA, et al. cacna2d3, a voltage-gated calcium channel subunit, functions in vertebrate habituation learning and the startle sensitivity threshold. PLOS ONE. 2022; 17: e0270903. https://doi.org/10.1371/journal.pone.0270903 PMID: 35834485

30. Marsden KC, Granato M. In Vivo Ca2+ Imaging Reveals that Decreased Dendritic Excitability Drives Startle Habituation. Cell Reports. 2015; 13: 1733–1740. https://doi.org/10.1016/j.celrep.2015.10.060 PMID: 26655893

31. Randlett O, Wee CL, Naumann EA, Nnaemeka O, Schoppik D, Fitzgerald JE, et al. Whole-brain activity mapping onto a zebrafish brain atlas. Nature Methods. 2015; 12: 1039–1046. https://doi.org/10.1038/nmeth.3581 PMID: 26778924

32. Meserve JH, Nelson JC, Marsden KC, Hsu J, Echeverry FA, Jain RA, et al. A forward genetic screen identifies Dolk as a regulator of startle magnitude through the potassium channel subunit Kv1.1. PLOS Genetics. 2021; 17: e1008943. https://doi.org/10.1371/journal.pgen.1008943 PMID: 34061829

33. Mouret RZ, Greenbaum JP, Doll HM, Brody EM, Iacobucci EL, Roland NC, et al. The Adaptor Protein 2 (AP2) complex modulates habituation and behavioral selection across multiple pathways and time windows. bioRxiv; 2022. p. 2022.05.20.492863. https://doi.org/10.1101/2022.05.20.492863

34. Pantoja C, Larsch J, Laurell E, Marquart G, Kunst M, Baier H. Rapid Effects of Selection on Brain-wide Activity and Behavior. Current Biology. 2020; 30: 3647–3656.e3. https://doi.org/10.1016/j.cub.2020.06.086 PMID: 32763165

35. Lange M, Norton W, Coolen M, Chaminade M, Merker S, Proft F, et al. The ADHD-linked gene Lphn3.1 controls locomotor activity and impulsivity in zebrafish. Molecular Psychiatry. 2012; 17: 855–855. https://doi.org/10.1038/mp.2012.119 PMID: 22918194

36. Fierro J, Haynes DR, Washbourne P. 4.1Ba is necessary for glutamatergic synapse formation in the sensorimotor circuit of developing zebrafish. PLoS One. 2018; 13: e0205255. https://doi.org/10.1371/journal.pone.0205255 PMID: 30286167

37. Bátora D, Zsigmond Á, Lőrincz IZ, Szegvári G, Varga M, Málnási-Csizmadia A. Subcellular Dissection of a Simple Neural Circuit: Functional Domains of the Mauthner-Cell During Habituation. Front Neural Circuits. 2021; 15. https://doi.org/10.3389/fncir.2021.648487 PMID: 33828462

38. Halberstadt AL, Geyer MA. Habituation and sensitization of acoustic startle: opposite influences of dopamine D1 and D2-family receptors. Neurobiol Learn Mem. 2009; 92: 243–248. https://doi.org/10.1016/j.nlm.2008.05.015 PMID: 18644244

39. García-González J, Brock AJ, Parker MO, Riley RJ, Joliffe D, Sudwarts A, et al. Identification of slit3 as a locus affecting nicotine preference in zebrafish and human smoking behaviour. Larhammar D, Stainier DY, Westberg L, Clark K, editors. eLife. 2020; 9: e51295. https://doi.org/10.7554/eLife.51295 PMID: 32209227

40. Barrios JP, Wang W-C, England R, Reifenberg E, Douglass AD. Hypothalamic Dopamine Neurons Control Sensorimotor Behavior by Modulating Brainstem Premotor Nuclei in Zebrafish. Current biology: CB. 2020; 30: 4606–4618.e4. https://doi.org/10.1016/j.cub.2020.09.002 PMID: 33007241

41. Godoy R, Hua K, Kalyn M, Cusson V-M, Anisman H, Ekker M. Dopaminergic neurons regenerate following chemogenetic ablation in the olfactory bulb of adult Zebrafish (Danio rerio). Sci Rep. 2020; 10: 1–12. https://doi.org/10.1038/s41598-020-69734-0 PMID: 32733000

42. Marsden KC, Jain RA, Wolman MA, Echeverry FA, Nelson JC, Hayer KE, et al. A Cyfip2-Dependent Excitatory Interneuron Pathway Establishes the Innate Startle Threshold. Cell Reports. 2018; 23: 878–887. https://doi.org/10.1016/j.celrep.2018.03.095 PMID: 29669291

43. Zhang X, Zhang Z, Zhao Q, Lou X. Rapid and Efficient Live Zebrafish Embryo Genotyping. Zebrafish. 2020; 17: 56–58. https://doi.org/10.1089/zeb.2019.1796 PMID: 31851585

44. Granato M, Furutani-Seiki M, Haffter P, Hammerschmidt M, Heisenberg C-P, Jiang Y-J, et al. Genes controlling and mediating locomotion behavior of the zebrafish embryo and larva. Development. 1996; 123: 399–413. https://doi.org/10.1242/dev.123.1.399 PMID: 9007258

45. Wee CL, Nikitchenko M, Wang W-C, Luks-Morgan SJ, Song E, Gagnon JA, et al. Zebrafish oxytocin neurons drive nocifensive behavior via brainstem premotor targets. Nat Neurosci. 2019; 22: 1477–1492. https://doi.org/10.1038/s41593-019-0452-x PMID: 31358991

46. R Core Team. R: A language and environment for statistical computing. Vienna, Austria: R Foundation for Statistical Computing; 2021. https://www.R-project.org/.

47. Wickham H, Averick M, Bryan J, Chang W, McGowan LD, François R, et al. Welcome to the Tidyverse. Journal of Open Source Software. 2019; 4: 1686. https://doi.org/10.21105/joss.01686

48. Kassambara A, Mundt F. factoextra: Extract and Visualize the Results of Multivariate Data Analyses. 2020. https://cran.r-project.org/web/packages/factoextra/readme/README.html.